

Chemical Reaction, Heat Source and Slip Effects on MHD Pulsatory Blood Flowing Past an Inclined Stenosed Artery Influenced by Body Acceleration

E. Amos¹, E. Omamoke² and Chinedu Nwaigwe¹

¹ Department of Mathematics, Rivers State University, Port Harcourt, Nigeria.

² Department of Mathematics, Bayelsa Medical University, Yenagoa, Nigeria.

Abstract - This study analyses the effects of chemical reaction, slip effect and heat source on the MHD flow of blood through an inclined permeable artery with stenosis under body acceleration present. The blood is treated as a non-Newtonian electrically conduction fluid with accumulated substances of fatty substance in the blood cells creating porosity at the artery walls. The mathematical model for the blood flow is developed with inclusion of buoyancy force for both energy and diffusion with variations in heat and mass transfer having an effect on the blood flow. The partial differential equation of the governing model is transformed to ordinary differential equation using the boundary conditions. Variations in parameters all had effects on the blood flow, temperature and diffusion. Results showed that chemical reaction, magnetic field and slip reduces the blood flow while the body acceleration, heat source and pressure gradient increases the blood flow.

Keywords - Magneto hydro dynamic (MHD), Slip Boundary, Chemical Reaction, Heat Source, Body Acceleration, Inclined porous artery.

I. INTRODUCTION

Blood is transported through the arteries of the blood vessels to various parts of the body from the heart as it beats. The nature of the vessel is elastic making it to possess some permeability and also porous. The blood flowing through the reddish arteries from the heart carries both nutrients and rich oxygen to the tissues in the body and removes waste products and carbon dioxide through the blood vessels, hence sustaining and keeping the tissues of the body healthy, Blessy and Summan [1]. Further findings revealed that the blood flowing through an artery in a human system is a problem of fluid dynamics with hemodynamics dealing with the progression and development of the stenosis in the arteries resulting to cardiovascular diseases. Ku [2] review showed that the cardiovascular system flow loops internally with circulation of blood taking place through the multiple branches with unsteady and viscous forces acting on the fluid. An abnormal response biologically called arteriosclerosis is created by an uncommon condition hemodynamically. The stenosis formed results to turbulent and reduced flow of blood with thrombosis occurring at the stenosis throat due to high shear stress which could block the flow of blood to the brain or the heart. As the heart beats, blood accelerates through the arteries creating a pressure gradient which causes the blood to flow in a pulsatile pattern. Allen et al. [3] studied the relevance of non-pulsatile and pulsatile blood flow in blood pump design. The pressure experiences pulsatile changes with blood flow accelerated (systole) and blood flow deceleration (diastole) such that at the walls of the artery, the energy stored keeps a pressure gradient that is positive, Pellerito [4]. Plaques in form of accumulated fats and others remain at the wall of the arteries which causes arteriosclerosis which blocks the arteries and prevent the free flow of blood past the arteries. Kumar [5] did a study on the pulsatile blood flow model of two-fluid passing through an artery that is narrow with stenosis present at the wall using a mathematical model for analysis. The erythrocyte is suspended at the Herschel Burlkley Newtonian fluid while the plasma is suspended at the peripheral Newtonian fluid layer. Results showed that for the two fluid model the increase in shear stress and flow resistance is low compared to a model of single fluid of Herschel Burlkley model with the functioning of the disease of the arterial system enhanced by the peripheral layer. Nehad et al. [6] studied the influence of a pulsatile pressure gradient with the magnatic field placed transversely on the blood flow that is unsteady flowing past cylindrical channel that is tapered and inclined. Slip induced at the wall of the artery plays a significant effect during blood flow since it helps in reducing the blood flow as a result of the relative movement between the external layers of the fluid and the surface of the artery wall. Lukendra et al. [7] did a study on the pulsatile blood flow past a permeable porous artery with mild



stenosis that is inclined and tapered with the results showing that an increase in the slip velocity results to an increase in the axial blood flow velocity and volumetric flow rate while the reverse was observed when the magnetic field was increased. Eldesoky [8] did a study on pulsatile unsteady incompressible blood flow past a medium that is porous influenced by a slip and body acceleration with magnetic field effect present with the results showing the important role of slip condition on spurt, skin shear and hysteresis. Body acceleration is the sudden change in the velocity of the Body that is moving. This sudden change could have a significant effect on the blood flowing through the artery with the presence of stenosis at the wall of the artery. Das and Saha, [9] developed a mathematical model to study the pulsatile blood flow past a medium that is porous with body acceleration influenced by a magnetic field placed transversely with the blood considered to be electrically conducting fluid and a Newtonian fluid with the study having a key role in biomedical engineering. Varun et al. [10] did a similar work with [9] but a cauterized artery with perturbation method used for the solution with the results showing that the axial velocity of the blood flow decreased with the increase in body acceleration. Prakash et al. [11] did a study analyzing the heat source effect on MHD flow of blood past an artery that is bifurcated with the blood treated as an unsteady Newtonian fluid. Kumar et al. [12] developed a mathematical model to study the effect of chemical reaction and heat source on MHD flow of blood through an artery that is bifurcated with an applied magnetic field. The blood is assumed to be a fluid that conducts electricity and is a Newtonian fluid. Omamoke and Amos [13] did a study analyzing chemical and heat source effects on MHD free convective flow of fluid past and inclined surface that is porous with the results showing that both heat source and chemical reaction increase increases the velocity profile. Omamoke et al. [14] studied the effect of heat source and thermal radiation on MHD flow of blood with a magnetic field applied with the research suggesting possible treatment for tumor and low blood pressure. Also, Omamoke and Amos [15] did further inclusion of chemical reaction effect to [14] to observe the effect on the blood flow. The research objectives is to study the effects of chemical reaction, heat source, body acceleration, induced slip and others on the blood flow velocity to ascertain possible treatment for hypothermia, hyperthermia and tumor growth.

Formulation of the Problem

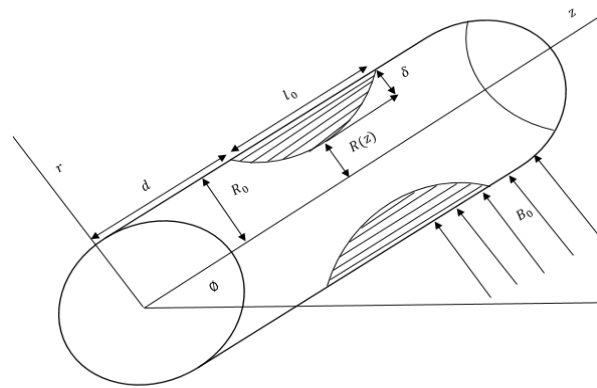


Figure 1: Geometry of the Blood Flow through the inclined artery

The blood which flows from the heart to various body muscles through the arteries is treated as a non-Newtonian electrically conducting viscous fluid with the walls of the artery been porous and stenosis present at the artery walls. From Figure 1, the artery is inclined at ϕ positioned at d with the length and height of stenosis defined as l_0 and δ . The blood is flowing in the axial direction z with the magnetic field B_0 placed perpendicularly to the artery whose radius and stenosis radius is R_0 and $R(z)$. The flow of the blood through the artery is assumed to be steady and unsteady with the governing equations developed for the momentum, energy and diffusion of the blood.

The stenosis formed in the artery is dependent on the location and height of the constriction at the wall of the artery. An electromagnetic force \vec{F} is created when the magnetic field is applied on blood since it is an electrical conducting fluid.

$$\vec{F} = q(\vec{E} + \vec{V} \times \vec{B})$$

(1) The current density \vec{j} is expressed as

$$\vec{J} = \sigma(\vec{E} + \vec{V} \times \vec{B}) \quad (2)$$

The total magnetic field intensity $B = B_0 + B_1$. A combination of the electric force and the magnetic force on the blood flow with electrical conductivity produces the Lorentz force with the electric field intensity vector \vec{E} negligible.

$$\vec{J} = \sigma(\vec{V} \times \vec{B}) \quad (3)$$

For small Reynolds number with the current density \vec{J} , the electromagnetic force F becomes

$$\vec{J} \times \vec{B} = -\sigma B_0^2 \vec{u} \quad (4)$$

Where $|B_0| = B_0$, F is the body force in the axial direction, $\vec{u} = (0,0,u)$ is the velocity vector distribution, $\vec{B} = (0, B_0, 0)$ is the magnetic field vector with the blood flow assumed to be steady and unsteady, axially symmetric and laminar with the study restricted to a one-dimensional blood flow in the axial direction of a coronary artery which is cylindrical in nature.

The flow geometry of the segmented stenotic artery with symmetrical shape in dimensional form proposed by Sankar [5] and Kumar et al. [12] is,

$$R(z') = \begin{cases} d'(z) - \frac{\delta'}{2} \left[1 + \cos \frac{2\pi}{l_0} \left\{ z' - d' - \frac{l'_0}{2} \right\} \right] \\ d'(z) \end{cases}, d' \leq z' \leq d' + l'_0 \quad (5)$$

The greatest height (R) of the stenosis happens at the center of the artery, Nadeem et al. [22]

Where $\xi = \tan \emptyset$ and $z = d + \frac{L_0}{s(\xi-1)}$ For $s \geq 2$

The mathematical expressions for the dimensional governing equations are

$$\rho \frac{\partial u'}{\partial t'} = -\frac{\partial p'}{\partial z'} + \rho G(t) + \frac{\mu}{r'} \frac{\partial}{\partial r'} \left(r' \frac{\partial u'}{\partial r'} \right) - \sigma_c B_0^2 u' + g \sin \emptyset - \frac{\mu}{k'_p} u' + \rho g B_T (T' - T_0) + \rho g B_C (C' - C_0) \quad (6)$$

$$\frac{\rho C_p}{k'_p} \left[\frac{\partial T'}{\partial t'} \right] = \frac{\partial^2 T'}{\partial r'^2} + \frac{1}{r'} \frac{\partial T'}{\partial r'} + \frac{Q_0 T'}{\rho C_p} \quad (7)$$

$$\emptyset \frac{\partial C'}{\partial t'} = \emptyset D' \left[\frac{\partial^2 C'}{\partial r'^2} + \frac{1}{r'} \frac{\partial C'}{\partial r'} \right] - E' (C' - C_0) \quad (8)$$

The initial and boundary slip conditions in dimensional are

$$\left. \begin{cases} \frac{\partial u'}{\partial r'} = -h' u', T' = T'_a, C' = C'_a \text{ at } r' = R'(z) \\ \frac{\partial u'}{\partial r'} = 0, \frac{\partial \theta'}{\partial r'} = 0, \frac{\partial C'}{\partial r'} = 0 \text{ at } r' = 0 \end{cases} \right\} \quad (10)$$

The pressure gradient in dimensional form is expressed as

$$-\frac{\partial p'}{\partial z'} = P_0 + P_1 \cos(w_p t'); t' \geq 0 \quad (11)$$

Where $w_p = 2\pi f_p$ and $w_b = 2\pi f_b$

The body acceleration in dimensional form

$$G'(t) = G'_0 \cos(w_b t' + \varphi); t' \geq 0 \quad (12)$$

The dimensionless variable is introduced include.

$$\begin{aligned} d(z') = R_0 + \xi z' \quad ; \quad \delta = \frac{\delta'}{R_0}, \quad u = \frac{u'}{u_0}; l_0 = \frac{l_0'}{R_0}; l_1 = \frac{d'}{R_0}; r = \frac{r'}{R_0}; z = \frac{z'}{R_0}; b = \frac{w_b}{w_p}; t = w_p t'; R(z) = \frac{R'(z)}{R_0}; P = \frac{R_0 \rho'}{u_0 \mu}; Re = \frac{\rho \omega R_0'^2}{\mu}; \theta = \frac{T' - T_0}{T'_w - T_0}; \theta_a = \frac{T'_a - T_0}{T'_w - T_0}; C = \frac{C' - C_\infty}{C'_w - C_\infty}; C_a = \frac{C'_a - C_\infty}{C'_w - C_\infty}; N^2 = \frac{R_0'^2 Q_0}{\rho c_p k'_p}; M^2 = \frac{\sigma R_0'^2 B_0^2}{\mu}; Pe = \frac{\rho R_0'^2 c_p}{k'_p}; Sc = \frac{\theta}{D'}; Kr = \frac{E' R_0'^2}{\theta D'}; G_r = \frac{g \rho R_0'^2 \beta_T \theta (T_w - T_0)}{u_0 \mu}; G_c = \frac{g \rho R_0'^2 \beta_C (C_w - C_0)}{u_0 \mu}; P_1 = \frac{P'_1 R_0'^2}{u_0 \mu}; P_0 = \frac{P'_0 R_0'^2}{u_0 \mu}; G_0 = \frac{\rho G'_0 R_0'^2}{u_0 \mu}; f_r = \frac{u_0 \mu}{g R_0'^2}; D = \frac{D'}{D_0}; k = \frac{k'_p}{R_0'^2}; h = h' R_0'; \end{aligned} \tag{13}$$

The dimensionless flow geometry with stenosis is expressed as, Sankar [5] and Kumar et al. [12]

$$R(z) = \left\{ \begin{aligned} & (1 + \xi z) - \frac{\delta}{2} \left[1 + \cos \frac{2\pi}{l_0} \left\{ z - l_1 - \frac{l_0}{2} \right\} \right] \\ & (1 + \xi z) \end{aligned} \right\}, l_1 \leq z \leq l_1 + l_0 \tag{14}$$

The dimensionless Pressure gradient

$$-\frac{\partial p}{\partial z} = P_0 + P_l \cos(w_p t); t \geq 0 \tag{15}$$

The body acceleration in dimensionless form

$$G(t) = G_0 \cos(w_b t + \varphi); t \geq 0 \tag{16}$$

The blood flow momentum, temperature and concentration equation in dimensionless form is written as for third consideration as:

$$Re \frac{\partial u}{\partial t} = P_0 + P_L \cos t + G_0 \cos(bt + \varphi) + \left(\frac{\partial^2 u}{\partial r^2} + \frac{1}{r} \frac{\partial u}{\partial r} \right) - \left(M^2 + \frac{1}{K} \right) u + \frac{\sin \theta}{Fr} + G_r \theta + G_c C \tag{17}$$

$$Pe \frac{\partial \theta}{\partial t} = \frac{\partial^2 \theta}{\partial r^2} + \frac{1}{r} \frac{\partial \theta}{\partial r} + N^2 \theta \tag{18}$$

$$ScRe \frac{\partial C}{\partial t} = \frac{\partial^2 C}{\partial r^2} + \frac{1}{r} \frac{\partial C}{\partial r} - KrC \tag{19}$$

The initial and boundary slip conditions are

$$\left. \begin{aligned} & \left(\frac{\partial u}{\partial r} = -hu, \theta = \theta_a, C = C_a \text{ at } r = R(z) \right) \\ & \left(\frac{\partial u}{\partial r} = 0, \frac{\partial \theta}{\partial r} = 0, \frac{\partial C}{\partial r} = 0 \text{ at } r = 0 \right) \end{aligned} \right\} \tag{20}$$

Solution to the Problem

The Frobenius method is applied to solve analytically the governing nonlinear second order differential equation with the solutions gotten for the steady and pulsatile blood flow velocity, temperature and mass diffusion in non-dimensional, expressed as.

$$u(r, t) = u_0(r) + u_p(r) \epsilon e^{i\omega t} \tag{21}$$

$$\theta(r, t) = \theta_0(r) + \theta_p(r) \epsilon e^{i\omega t} \tag{22}$$

$$C(r, t) = C_0(r) + C_p(r) \epsilon e^{i\omega t} \tag{23}$$

The steady and pulsatile state for the concentration is expressed below as

$$\frac{\partial^2 C_0}{\partial r^2} + \frac{1}{r} \frac{\partial C_0}{\partial r} - KrC_0 = 0 \tag{24}$$

$$\frac{\partial^2 C_p}{\partial r^2} + \frac{1}{r} \frac{\partial C_p}{\partial r} - \alpha_2 C_p = 0 \tag{25}$$

$$\alpha_2 = Kr - i\omega Pe$$

The steady and pulsatile state for the temperature is expressed below as

$$\frac{\partial^2 \theta_0}{\partial r^2} + \frac{1}{r} \frac{\partial \theta_0}{\partial r} + N^2 \theta_0 = 0 \tag{26}$$

$$\frac{\partial^2 \theta_p}{\partial r^2} + \frac{1}{r} \frac{\partial \theta_p}{\partial r} + \alpha_1 \theta_p = 0 \tag{27}$$

$$\text{Where } \alpha_1 = N^2 - i\omega Pe$$

The steady and pulsatile state for the blood flow velocity is expressed below as

$$\frac{\partial^2 u_0}{\partial r^2} + \frac{1}{r} \frac{\partial u_0}{\partial r} - \beta_1 u_0 = -G - G_r \theta_0 - G_c C_0 \tag{28}$$

$$\frac{\partial^2 u_p}{\partial r^2} + \frac{1}{r} \frac{\partial u_p}{\partial r} - \beta_2 u_p = -F - G_r \theta_p - G_c C_p \tag{29}$$

$$\beta_1 = M^2 + \frac{1}{K}; G = P_0 + \frac{\sin \phi}{Fr}; \beta_2 = M^2 + \frac{1}{K} + Re i\omega \text{ and } F = P_1 \cos t + G_0 \cos(bt + \phi)$$

The steady state and pulsatile state solutions for both the concentration, temperature and flow velocity is gotten by adopting Funch's theorem, also known as the Frobenius power series expressed as

$$C_0(r) = \sum_{n=0}^{\infty} a_n r^{n+k} \text{ Where } a_n, k \in C_1 \tag{30}$$

$$C_p(r) = \sum_{n=0}^{\infty} b_n r^{m+k} \text{ Where } b_m, k \in C_2 \tag{31}$$

$$\theta_0(r) = \sum_{n=0}^{\infty} c_n r^{n+k} \text{ Where } c_n, k \in C_3 \tag{32}$$

$$\theta_p(r) = \sum_{n=0}^{\infty} d_n r^{m+k} \text{ Where } d_m, k \in C_4 \tag{33}$$

$$u_0 = \sum_{n=0}^{\infty} e_n r^{n+k} \text{ Where } e_n, k \in C_3 \tag{34}$$

$$u_p = \sum_{m=0}^{\infty} f_m r^{m+k} \text{ Where } f_m, k \in C_4 \tag{35}$$

The mathematical expression for the concentration in steady state is

$$C_0 = C_1 \left[1 + \frac{Kr r^2}{2^2} + \frac{Kr^2 r^4}{2^2 4^2} + \frac{Kr^3 r^6}{2^2 4^2 6^2} + \frac{Kr^4 r^8}{2^2 4^2 6^2 8^2} + \dots \right] + D_1 \left[\ln r \left(1 + \frac{Kr r^2}{2^2} + \frac{Kr^2 r^4}{2^2 4^2} + \frac{Kr^3 r^6}{2^2 4^2 6^2} + \frac{Kr^4 r^8}{2^2 4^2 6^2 8^2} + \dots \right) + \left(-\frac{Kr r^2}{2^2} - \frac{3Kr^2 r^4}{2^3 4^2} - \frac{Kr^3 r^6}{4^3 6^3} + \frac{Kr^4 r^8}{2^5 6^3 8^3} - \dots \right) \right] \tag{36}$$

With $D_1 = 0$ and applying the boundary condition in equation (20) to equation (36), then

$$C_0 = C_1 \left[1 + \frac{Kr r^2}{2^2} + \frac{Kr^2 r^4}{2^2 4^2} + \frac{Kr^3 r^6}{2^2 4^2 6^2} + \frac{Kr^4 r^8}{2^2 4^2 6^2 8^2} + \dots \right] \tag{37}$$

$$C_1 = \frac{C_R}{\left[1 + \frac{Kr R^2}{2^2} + \frac{Kr^2 R^4}{2^2 4^2} + \frac{Kr^3 R^6}{2^2 4^2 6^2} + \frac{Kr^4 R^8}{2^2 4^2 6^2 8^2} + \dots\right]} \quad (38)$$

The mathematical expression for the concentration in pulsatile state is

$$C_p = C_2 \left[1 + \frac{\alpha_2 r^2}{2^2} + \frac{\alpha_2^2 r^4}{2^2 4^2} + \frac{\alpha_2^3 r^6}{2^2 4^2 6^2} + \frac{\alpha_2^4 r^8}{2^2 4^2 6^2 8^2} + \dots\right] + D_2 \left[\ln r \left(1 + \frac{\alpha_2 r^2}{2^2} + \frac{\alpha_2^2 r^4}{2^2 4^2} + \frac{\alpha_2^3 r^6}{2^2 4^2 6^2} + \frac{\alpha_2^4 r^8}{2^2 4^2 6^2 8^2} + \dots\right) + \left(\frac{\alpha_2 r^2}{2^2} + \frac{3\alpha_2^2 r^4}{2^3 4^2} + \frac{\alpha_2^3 r^6}{4^3 6^3} + \frac{\alpha_2^4 r^8}{2^5 6^3 8^3} - \dots\right)\right] \quad (39)$$

With $D_2 = 0$ and applying the boundary condition in equation (20) to equation (39), then

$$C_p = C_2 \left[1 + \frac{\alpha_2 r^2}{2^2} + \frac{\alpha_2^2 r^4}{2^2 4^2} + \frac{\alpha_2^3 r^6}{2^2 4^2 6^2} + \frac{\alpha_2^4 r^8}{2^2 4^2 6^2 8^2} + \dots\right] \quad (40)$$

$$C_2 = \frac{C_R}{\left[1 + \frac{\alpha_2 R^2}{2^2} + \frac{\alpha_2^2 R^4}{2^2 4^2} + \frac{\alpha_2^3 R^6}{2^2 4^2 6^2} + \frac{\alpha_2^4 R^8}{2^2 4^2 6^2 8^2} + \dots\right]} \quad (41)$$

The mathematical expression for the temperature in the steady state is

$$\theta_0 = C_3 \left[1 - \frac{N^2 r^2}{2^2} + \frac{N^4 r^4}{2^2 4^2} - \frac{N^6 r^6}{2^2 4^2 6^2} + \frac{N^8 r^8}{2^2 4^2 6^2 8^2} + \dots\right] + D_3 \left[\ln r \left(1 - \frac{N^2 r^2}{2^2} + \frac{N^4 r^4}{2^2 4^2} - \frac{N^6 r^6}{2^2 4^2 6^2} + \frac{N^8 r^8}{2^2 4^2 6^2 8^2} + \dots\right) + \left(\frac{N^2 r^2}{2^2} - \frac{3N^4 r^4}{2^3 4^2} + \frac{N^6 r^6}{4^3 6^3} + \frac{N^8 r^8}{2^5 6^3 8^3} - \dots\right)\right] \quad (42)$$

With $D_3 = 0$ and applying the boundary condition in equation (20) to equation (42), then

$$\theta_0 = C_3 \left[1 - \frac{N^2 r^2}{2^2} + \frac{N^4 r^4}{2^2 4^2} - \frac{N^6 r^6}{2^2 4^2 6^2} + \frac{N^8 r^8}{2^2 4^2 6^2 8^2} + \dots\right] \quad (43)$$

$$C_3 = \frac{\theta_R}{\left[1 - \frac{N^2 R^2}{2^2} + \frac{N^4 R^4}{2^2 4^2} - \frac{N^6 R^6}{2^2 4^2 6^2} + \frac{N^8 R^8}{2^2 4^2 6^2 8^2} + \dots\right]} \quad (44)$$

The mathematical expression for the temperature in the pulsatile state is expressed as

$$\theta_p = C_4 \left[1 - \frac{\alpha_1 r^2}{2^2} + \frac{\alpha_1^2 r^4}{2^2 4^2} - \frac{\alpha_1^3 r^6}{2^2 4^2 6^2} + \frac{\alpha_1^4 r^8}{2^2 4^2 6^2 8^2} + \dots\right] + D_4 \left[\ln r \left(1 - \frac{\alpha_1 r^2}{2^2} + \frac{\alpha_1^2 r^4}{2^2 4^2} - \frac{\alpha_1^3 r^6}{2^2 4^2 6^2} + \frac{\alpha_1^4 r^8}{2^2 4^2 6^2 8^2} + \dots\right) + \left(\frac{\alpha_1 r^2}{2^2} - \frac{3\alpha_1^2 r^4}{2^3 4^2} + \frac{\alpha_1^3 r^6}{4^3 6^3} + \frac{\alpha_1^4 r^8}{2^5 6^3 8^3} - \dots\right)\right] \quad (45)$$

With $D_4 = 0$ and applying the boundary condition in equation (20) to equation (45), then

$$\theta_p = C_4 \left[1 - \frac{\alpha_1 r^2}{2^2} + \frac{\alpha_1^2 r^4}{2^2 4^2} - \frac{\alpha_1^3 r^6}{2^2 4^2 6^2} + \frac{\alpha_1^4 r^8}{2^2 4^2 6^2 8^2} + \dots\right] \quad (46)$$

$$C_4 = \frac{\theta_R}{\left[1 - \frac{\alpha_1 R^2}{2^2} + \frac{\alpha_1^2 R^4}{2^2 4^2} - \frac{\alpha_1^3 R^6}{2^2 4^2 6^2} + \frac{\alpha_1^4 R^8}{2^2 4^2 6^2 8^2} + \dots\right]} \quad (47)$$

The expression for temperature in equation (23) is obtained by combining equation (37) and (40)

$$C(r, t) = C_1 \left[1 + \frac{Kr r^2}{2^2} + \frac{Kr^2 r^4}{2^2 4^2} + \frac{Kr^3 r^6}{2^2 4^2 6^2} + \frac{Kr^4 r^8}{2^2 4^2 6^2 8^2} + \dots\right] + \left(C_2 \left[1 + \frac{\alpha_2 r^2}{2^2} + \frac{\alpha_2^2 r^4}{2^2 4^2} + \frac{\alpha_2^3 r^6}{2^2 4^2 6^2} + \frac{\alpha_2^4 r^8}{2^2 4^2 6^2 8^2} + \dots\right]\right) \epsilon e^{i\omega t} \quad (48)$$

The expression for temperature in equation (22) is obtained by combining equation (43) and (48)

$$\theta(r, t) = C_3 \left[1 - \frac{N^2 r^2}{2^2} + \frac{N^4 r^4}{2^2 4^2} - \frac{N^6 r^6}{2^2 4^2 6^2} + \frac{N^8 r^8}{2^2 4^2 6^2 8^2} + \dots \right] + \left(C_4 \left[1 - \frac{\alpha_1 r^2}{2^2} + \frac{\alpha_1^2 r^4}{2^2 4^2} - \frac{\alpha_1^3 r^6}{2^2 4^2 6^2} + \frac{\alpha_1^4 r^8}{2^2 4^2 6^2 8^2} + \dots \right] \right) \epsilon e^{i\omega t} \quad (49)$$

The expression for the complementary solution for flow velocity in steady state from equation (28) is

$$u_{0c} = C_5 \left[1 + \frac{\beta_1 r^2}{2^2} + \frac{\beta_1^2 r^4}{2^2 4^2} + \frac{\beta_1^3 r^6}{2^2 4^2 6^2} + \frac{\beta_1^4 r^8}{2^2 4^2 6^2 8^2} + \dots \right] + D_5 \left[\ln r \left(1 + \frac{\beta_1 r^2}{2^2} + \frac{\beta_1^2 r^4}{2^2 4^2} + \frac{\beta_1^3 r^6}{2^2 4^2 6^2} + \frac{\beta_1^4 r^8}{2^2 4^2 6^2 8^2} + \dots \right) + \left(-\frac{\beta_1 r^2}{2^2} - \frac{3\beta_1^2 r^4}{2^3 4^2} - \frac{\beta_1^3 r^6}{4^3 6^3} + \frac{\beta_1^4 r^8}{2^5 6^3 8^3} - \dots \right) \right] \quad (50)$$

With $D_5 = 0$ and applying the boundary condition in equation (20) to equation (50), then

$$u_{0c} = C_5 \left[1 + \frac{\beta_1 r^2}{2^2} + \frac{\beta_1^2 r^4}{2^2 4^2} + \frac{\beta_1^3 r^6}{2^2 4^2 6^2} + \frac{\beta_1^4 r^8}{2^2 4^2 6^2 8^2} + \dots \right] \quad (51)$$

The expression for the complementary solution for flow velocity in pulsatile state from equation (28) is

$$u_{0p} = S_0 + S_1 r^2 + S_2 r^4 + S_3 r^6 + S_4 r^8 \quad (52)$$

The flow velocity solution in equation (28) is the combination of equation (51) and (52).

$$u_0 = C_5 \left[1 + \frac{\beta_1 r^2}{2^2} + \frac{\beta_1^2 r^4}{2^2 4^2} + \frac{\beta_1^3 r^6}{2^2 4^2 6^2} + \frac{\beta_1^4 r^8}{2^2 4^2 6^2 8^2} + \dots \right] + S_0 + S_1 r^2 + S_2 r^4 + S_3 r^6 + S_4 r^8 \quad (53)$$

Where $C_5 = -$

$$\frac{[h(S_0 + S_1 R^2 + S_2 R^4 + S_3 R^6 + S_4 R^8) + 2S_1 R + 4S_2 R^3 + 6S_3 R^5 + 8S_4 R^7]}{\left[\frac{\beta_1 R^2}{2} + \frac{\beta_1^2 R^3}{2^2 4} + \frac{\beta_1^3 R^5}{2^2 4^2 6} + \frac{\beta_1^4 R^7}{2^2 4^2 6^2 8} + \dots \right] + h \left[1 + \frac{\beta_1 R^2}{2^2} + \frac{\beta_1^2 R^4}{2^2 4^2} + \frac{\beta_1^3 R^6}{2^2 4^2 6^2} + \frac{\beta_1^4 R^8}{2^2 4^2 6^2 8^2} + \dots \right]}$$

The expression of the complementary solution for the flow velocity in pulsatile state in equation (29) is

$$u_{pc} = C_6 \left[1 + \frac{\beta_2 r^2}{2^2} + \frac{\beta_2^2 r^4}{2^2 4^2} + \frac{\beta_2^3 r^6}{2^2 4^2 6^2} + \frac{\beta_2^4 r^8}{2^2 4^2 6^2 8^2} + \dots \right] + D_6 \left[\ln r \left(1 + \frac{\beta_2 r^2}{2^2} + \frac{\beta_2^2 r^4}{2^2 4^2} + \frac{\beta_2^3 r^6}{2^2 4^2 6^2} + \frac{\beta_2^4 r^8}{2^2 4^2 6^2 8^2} + \dots \right) + \left(-\frac{\beta_2 r^2}{2^2} - \frac{3\beta_2^2 r^4}{2^3 4^2} - \frac{\beta_2^3 r^6}{4^3 6^3} + \frac{\beta_2^4 r^8}{2^5 6^3 8^3} - \dots \right) \right] \quad (54)$$

With $D_6 = 0$ and applying the boundary condition in equation (20) to equation (54), then

$$u_{pc} = C_6 \left[1 + \frac{\beta_2 r^2}{2^2} + \frac{\beta_2^2 r^4}{2^2 4^2} + \frac{\beta_2^3 r^6}{2^2 4^2 6^2} + \frac{\beta_2^4 r^8}{2^2 4^2 6^2 8^2} + \dots \right] \quad (55)$$

The expression of particular solution for the flow velocity in pulsatile state from equation (29) is

$$u_{pp} = T_0 + T_1 r^2 + T_2 r^4 + T_3 r^6 + T_4 r^8 \quad (56)$$

The flow velocity solution in equation (28) is the combination of equation (55) and (56).

$$u_p = C_6 \left[1 + \frac{\beta_2 r^2}{2^2} + \frac{\beta_2^2 r^4}{2^2 4^2} + \frac{\beta_2^3 r^6}{2^2 4^2 6^2} + \frac{\beta_2^4 r^8}{2^2 4^2 6^2 8^2} + \dots \right] + T_0 + T_1 r^2 + T_2 r^4 + T_3 r^6 + T_4 r^8 \quad (57)$$

Where $C_6 = -$

$$\frac{[h(T_0+T_1R^2+T_2R^4+T_3R^6+T_4R^8)+2T_1R+4T_2R^3+6T_3R^5+8T_4R^7]}{\left[\frac{\beta_2 R^2}{2} + \frac{\beta_2^2 R^3}{2^2 4} + \frac{\beta_2^3 R^5}{2^2 4^2 6} + \frac{\beta_2^4 R^7}{2^2 4^2 6^2 8} + \dots\right]} + h\left[1 + \frac{\beta_2 R^2}{2^2} + \frac{\beta_2^2 R^4}{2^2 4^2} + \frac{\beta_2^3 R^6}{2^2 4^2 6^2} + \frac{\beta_2^4 R^8}{2^2 4^2 6^2 8^2} + \dots\right]$$

The blood flow velocity solution is obtained by substituting equation (53) and (57) into equation (21) is expressed as

$$u(r, t) = C_5 \left[1 + \frac{\beta_1 r^2}{2^2} + \frac{\beta_1^2 r^4}{2^2 4^2} + \frac{\beta_1^3 r^6}{2^2 4^2 6^2} + \frac{\beta_1^4 r^8}{2^2 4^2 6^2 8^2} + \dots \right] + S_0 + S_1 r^2 + S_2 r^4 + S_3 r^6 + S_4 r^8 + \left(C_6 \left[1 + \frac{\beta_2 r^2}{2^2} + \frac{\beta_2^2 r^4}{2^2 4^2} + \frac{\beta_2^3 r^6}{2^2 4^2 6^2} + \frac{\beta_2^4 r^8}{2^2 4^2 6^2 8^2} + \dots \right] + T_0 + T_1 r^2 + T_2 r^4 + T_3 r^6 + T_4 r^8 \right) \epsilon e^{i\omega t} \tag{58}$$

The Solution for the Fluid Acceleration equation

$$F(r, t) = \frac{du}{dt} = i\omega \epsilon e^{i\omega t} \left(C_6 \left[1 + \frac{\beta_2 r^2}{2^2} + \frac{\beta_2^2 r^4}{2^2 4^2} + \frac{\beta_2^3 r^6}{2^2 4^2 6^2} + \frac{\beta_2^4 r^8}{2^2 4^2 6^2 8^2} + \dots \right] + \frac{4T_1}{\beta_2} + \frac{GrC_2}{\beta_2} + \frac{GcC_4}{\beta_2} + T_1 r^2 + T_2 r^4 + T_3 r^6 + T_4 r^8 \right) + \epsilon e^{i\omega t} \frac{P_1}{\beta_2} (i\omega \cos t - \sin t) + \epsilon e^{i\omega t} \frac{G_0}{\beta_2} (i\omega \cos(bt + \varphi) - b \sin(bt + \varphi)) \tag{59}$$

The Solution for the Wall Shear Stress equation

$$\frac{du}{dr} = C_5 \left[\frac{\beta_1 r}{2} + \frac{\beta_1^2 r^3}{2^2 4} + \frac{\beta_1^3 r^5}{2^2 4^2 6} + \frac{\beta_1^4 r^7}{2^2 4^2 6^2 8} + \dots \right] + 2S_1 r + 4S_2 r^3 + 6S_3 r^5 + 8S_4 r^7 + \left(C_{10} \left[\frac{\beta_2 r}{2^2} + \frac{\beta_2^2 r^3}{2^2 4} + \frac{\beta_2^3 r^5}{2^2 4^2 6} + \frac{\beta_2^4 r^7}{2^2 4^2 6^2 8} + \dots \right] + 2T_1 r + 4T_2 r^3 + 6T_3 r^5 + 8T_4 r^7 \right) \epsilon e^{i\omega t} \tag{60}$$

The Solution for the Volumetric Flow Rate equation

$$Q(r, t) = 2\pi \int_0^a r u(r, t) dr = 2\pi \left\{ C_5 \left[\frac{a^2}{2} + \frac{\beta_1 a^4}{2^2 4} + \frac{\beta_1^2 a^6}{2^2 4^2 6} + \frac{\beta_1^3 a^8}{2^2 4^2 6^2 8} + \frac{\beta_1^4 a^{10}}{2^2 4^2 6^2 8^2 10} + \dots \right] + \frac{S_0 a^2}{2} + \frac{S_1 a^4}{4} + \frac{S_2 a^6}{6} + \frac{S_3 a^8}{8} + \frac{S_4 a^{10}}{10} + \left(C_6 \left[\frac{a^2}{2} + \frac{\beta_2 a^4}{2^2 4} + \frac{\beta_2^2 a^6}{2^2 4^2 6} + \frac{\beta_2^3 a^8}{2^2 4^2 6^2 8} + \frac{\beta_2^4 a^{10}}{2^2 4^2 6^2 8^2 10} + \dots \right] + \frac{T_0 a^2}{2} + \frac{T_1 a^4}{4} + \frac{T_2 a^6}{6} + \frac{T_3 a^8}{8} + \frac{T_4 a^{10}}{10} \right) \epsilon e^{i\omega t} \right\} \tag{61}$$

II. GRAPHICAL RESULTS AND DISCUSSION

Observations from figure 4.1, shows that an increase in the inclination of the artery with values of $\phi = 15^\circ, 30^\circ, 45^\circ, 60^\circ$ where ϕ ranges from $15^\circ \leq \phi \leq 60^\circ$, causes the blood flow velocity to increase at the center but converges towards zero at the wall of the artery with stenosis. This implies that at different positions of the body at different angles, the blood flow will improve which will help to reduce ache and pains that could be experienced in the body as a result of the decrease in the flow of blood transported to various parts of the body. The same trend was observed for the blood acceleration in figure 4.2 while an irregular trend was observed for the volumetric flow rate in figure 4.3. It was observed in Figure 4.4 that as the body acceleration G_0 increased for values of $G_0 = 2, 5, 7, 9$ where G_0 ranges from $2 \leq G_0 \leq 9$, the blood flow velocity increased at the center of the artery but converges toward zero at the wall of the artery with stenosis. This is because, the body acceleration reduces the resistance of the blood flow which results to an increase in the blood flow velocity Sinha et al. [16]. Also, the increase in the velocity is as a result of an increase in both pulse rate and heart beat due to an increase in the body acceleration which causes the heart to pump more blood to the muscles Nadal and Kumari [17]. Similar effect was observed for the blood acceleration, shear stress and volumetric flow rate in figure 4.5, 4.6 and 4.7. It was observed in figure 4.8, that an increase in the magnetic field M of the artery with values of $M = 0.75, 1.0, 1.5, 2.0$ where M ranges from $0.75 \leq M \leq 2.0$, causes the velocity of the blood flow to decrease at the center of the artery but converges towards zero at the wall of the artery with stenosis. This occurs due to the magnetization which causes a rotating motion of the blood flow particles this is charged. This persistent rotating motion of the blood flowing with the charged particles results to a red blood cells suspension in the blood plasma resulting to the internal viscosity increase of the red blood cells. This increase of the internal viscosity of the blood results to an increase of the Lorentz force which will opposes, resist or inhibit the motion or flow of the blood particles. Similar results with discussions was done by Sharma et al. [18] and Kumar et al. [19]. Similar effect was observed for the blood acceleration, shear stress, volumetric flow

rate and concentration in figure 4.9, 4.10, 4.11 and 4.12. It was observed in figure 4.13, that the increase in the permeability of the medium k which is porous for values of $k = 0.5, 1.0, 2.0, 3.0$, where k ranges from $0.5 \leq k \leq 3.0$, caused the blood flow velocity to increase at the center of the artery but converges towards zero at the wall of the artery with stenosis. The slip at the artery wall slightly enhances the velocity while the reduction in the permeability of the medium which is porous actually controls the blood flow rate Eldesoky [8], Nadal and Kumari [17]. Similar effect was observed for the blood acceleration, shear stress and volumetric flow rate in figure 4.14, 4.15 and 4.16. From figure 4.17, it is observed that an increase in the pulsatile pressure gradient Pl for values of $Pl = 2, 4, 6, 8$, where Pl ranges from $2 \leq Pl \leq 8$, will cause the velocity of the blood flow to increase at the center of the artery but converges towards zero at the wall of the artery with stenosis. An increase in the pressure would lead to increase in the work rate and load the heart carries which could cause cardiac failure. Furthermore, the velocity increase due to conditions of high pressure will force the fluid to flow at a higher speed. Sinha et al. [20], Ogulu & Amos [21] and Sharma et al. [18]. Similar effect was observed for the blood acceleration, shear stress and volumetric flow rate in figure 4.18, 4.19 and 4.20. It was observed in figure 4.21, that an increase in the slip h for values of $h = 0.5, 1.0, 1.5, 2.0$, where h ranges from $0.5 \leq h \leq 2.0$, will cause the blood flow velocity to decrease at the center of the artery. Similar effect was observed for the blood acceleration and volumetric flow rate in figure 4.22 and 4.23 but an increase in the wall shear stress in figure 4.24. It was observed in values 4.25, that the increase in the artery radius with stenosis R for values of $R = 0.2, 0.3, 0.5, 0.7$, where R ranges from $0.2 \leq R \leq 0.7$, will cause the velocity of the blood flowing in the axial direction to increase at the center of the artery. Similar effect was observed for the blood acceleration and volumetric flow rate in figure 4.26 and 4.28 but a decrease in the wall shear stress in figure 4.27. It was observed in figure 4.29, that the increase in heat source H for values of $H = 1.0, 1.5, 2.0, 2.5$, where t ranges from $1 \leq H \leq 2.5$ in the second consideration, will cause the blood flow velocity in the axial direction to slightly increase. Similar effect was observed for the blood acceleration and the temperature in figure 4.30 and 4.31. It was observed in figure 4.32, that an increase in Peclet number Pe for values of $Pe = 2, 5, 7, 10$, where Pe ranges from $2 \leq Pe \leq 10$ in the second consideration, will cause the blood flow velocity in the axial direction to decrease. Similar effect was observed for the blood acceleration, shear stress and volumetric flow rate in figure 4.33, 4.34 and 4.35. It was observed in figure 4.36, it is observed that the increase in Grashof temperature number Gr for values of $Gr = 0.25, 0.5, 1, 1.25$, where Gr ranges from $0.25 \leq Gr \leq 1.25$ in the second consideration, will cause the blood velocity flowing in the axial direction to increase. This occurs as a result of the increase in the boussinesq source. The Grashof temperature number slows or reduces the relational effect of the force of thermal buoyancy to the force of hydrodynamic viscosity at the walls of the artery. Similar effect was observed for the blood acceleration, shear stress and volumetric flow rate in figure 4.37, 4.38 and 4.39. It was observed in figure 4.40, that the increase in the Grashof diffusion number Gc for values of $Gc = 0.25, 0.5, 1, 1.25$, where Gc ranges from $0.25 \leq Gc \leq 1.25$, will cause the velocity of the blood flow moving axially to increase. Similar effect was observed for the blood acceleration, shear stress and volumetric flow rate in figure 4.41, 4.42 and 4.43. From figure 4.44, it is observed that an increase in chemical reaction Kr for values of $Kr = 1, 3, 5, 7$, where Kr ranges from $1 \leq Kr \leq 7$, will cause the blood flow velocity in the axial direction to decrease. Similar behavior was observed for the blood acceleration, volumetric flow rate and concentration in figure 4.45, 4.47 and 4.48 but figure 4.46 showed a reverse behavior with an increase in shear stress at the artery walls. Some of the results agreed with study done by Bunonyo and Amos [23].

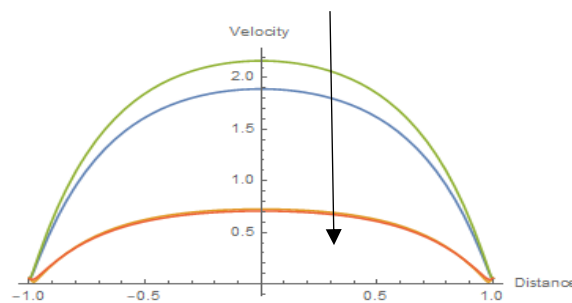


Figure 4.1 Graph for the velocity of Blood flow with increasing values of inclined artery $\phi = 15^{\circ}, 30^{\circ}, 45^{\circ}, 60^{\circ}$, when $Sc = 1, Kr = 1, Gc = 3, Gr = 2, H = 0.5, Pe = 1, Po = 2, Pl = 4, Go = 3, Fr = 0.05, b = 2, \beta = 30^{\circ}, k = 0.1, \alpha = 1, h = 1, R = 0.55, M = 1.5, \xi = 0.1, \omega = 1, t = 1$.

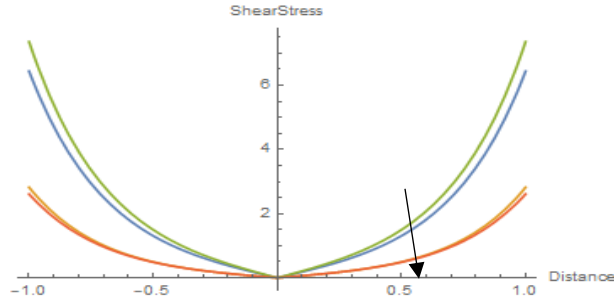


Figure 4.2 Graph for the shear stress at the wall with increasing values of inclined artery $\phi = 15^{\circ}, 30^{\circ}, 45^{\circ}, 60^{\circ}$, when $Sc = 1, Kr = 1, Gc = 3, Gr = 2, H = 0.5, Pe = 1, Po = 2, Pl = 4, Go = 3, Fr = 0.05, b = 2, \beta = 30^{\circ}, k = 0.1, \alpha = 1, h = 1, R = 0.55, M = 1.5, a = 1, \xi = 0.1, \omega = 1, t = 1$

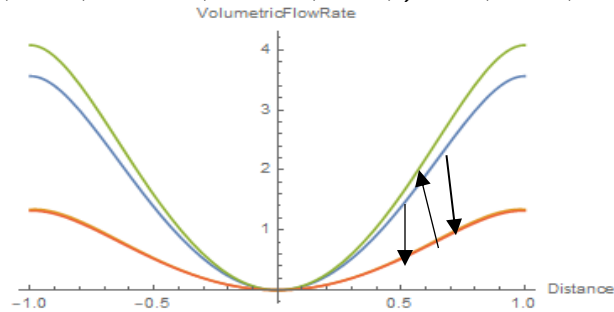


Figure 4.3 Graph for the Volumetric Flow rate with increasing values of inclined artery $\phi = 15^{\circ}, 30^{\circ}, 45^{\circ}, 60^{\circ}$, when $Sc = 1, Kr = 1, Gc = 3, Gr = 2, H = 0.5, Pe = 1, Po = 2, Pl = 4, Go = 3, Fr = 0.05, b = 2, \beta = 30^{\circ}, k = 0.1, \alpha = 1, h = 1, R = 0.55, M = 1.5, a = 1, \xi = 0.1, \omega = 1, t = 1$.

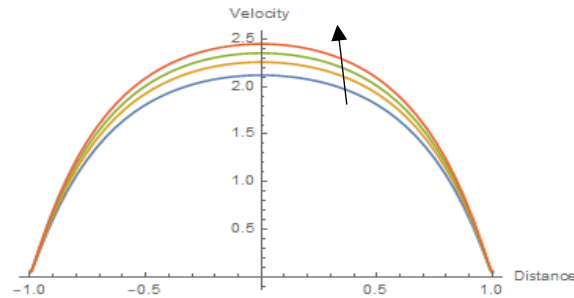


Figure 4.4 Graph for the velocity of Blood flow with increasing values of Body acceleration $Go = 2, 5, 7, 9$, when $Sc = 1, Kr = 1, Gc = 3, Gr = 2, H = 0.5, Pe = 1, Po = 2, Pl = 4, Fr = 0.05, b = 2, \phi = 30^{\circ}, \beta = 30^{\circ}, k = 0.1, \alpha = 1, h = 1, R = 0.55, M = 1.5, \xi = 0.1, \omega = 1, t = 1$.

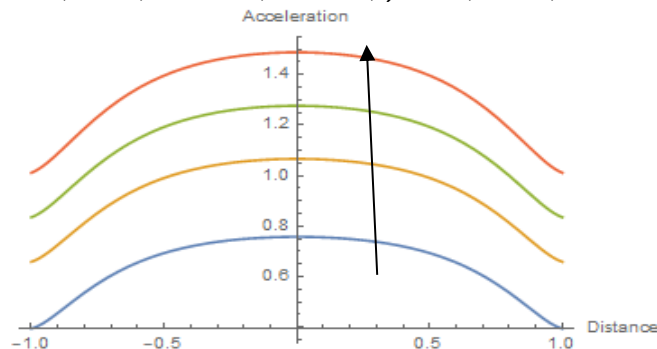


Figure 4.5 Graph for the Blood acceleration with increasing values of Body acceleration $Go = 2, 5, 7, 9$, when $Sc = 1, Kr = 1, Gc = 3, Gr = 2, H = 0.5, Pe = 1, Po = 2, Pl = 4, Fr = 0.05, b = 2, \beta = 30^{\circ}, k = 0.1, \alpha = 1, h = 1, R = 0.55, M = 1.5, \xi = 0.1, \omega = 1, t = 1$.

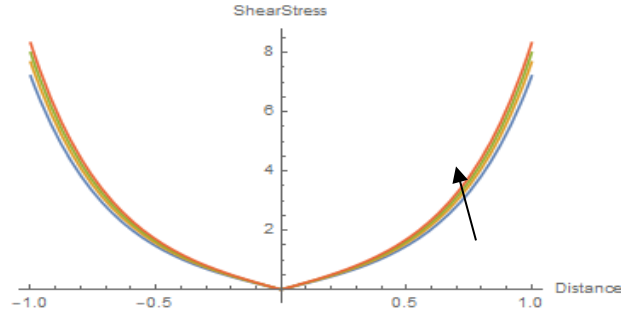


Figure 4.6 Graph for the shear stress at the wall with increasing values of Body acceleration $Go = 2, 5, 7, 9$, when $Sc = 1, Kr = 1, Gc = 3, Gr = 2, H = 0.5, Pe = 1, Po = 2, Pl = 4, Fr = 0.05, b = 2, \phi = 30^0, \beta = 30^0, k = 0.1, \alpha = 1, h = 1, R = 0.55, M = 1.5, a = 1, \xi = 0.1, \omega = 1, t = 1$.

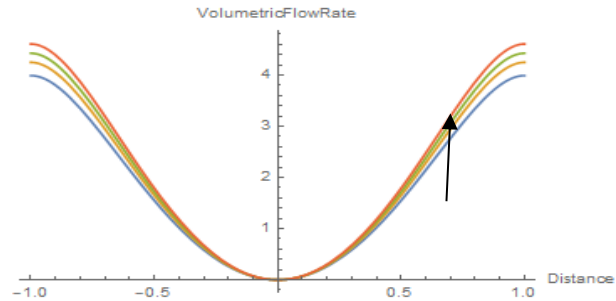


Figure 4.7 Graph for the Volumetric Flow rate with increasing values of Body acceleration $Go = 2, 5, 7, 9$, when $Sc = 1, Kr = 1, Gc = 3, Gr = 2, H = 0.5, Pe = 1, Po = 2, Pl = 4, Fr = 0.05, b = 2, \phi = 30^0, \beta = 30^0, k = 0.1, \alpha = 1, h = 1, R = 0.55, M = 1.5, \xi = 0.1, \omega = 1, t = 1$.

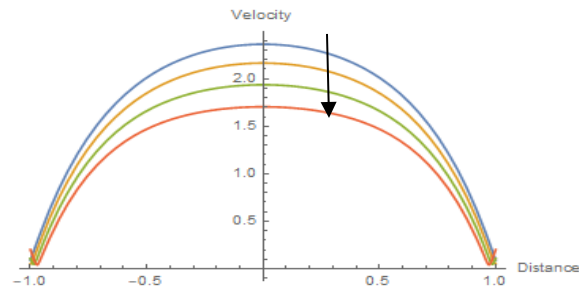


Figure 4.8 Graph for the velocity of Blood flow with increasing values of Magnetic field $M = 0.75, 1, 1.25, 1.5$, when $Sc = 1, Kr = 1, Gc = 3, Gr = 2, H = 0.5, Pe = 1, Po = 2, Pl = 4, Go = 3, Fr = 0.05, b = 2, \phi = 30^0, \beta = 30^0, k = 0.1, \alpha = 1, h = 1, R = 0.55, \xi = 0.1, \omega = 1, t = 1$.

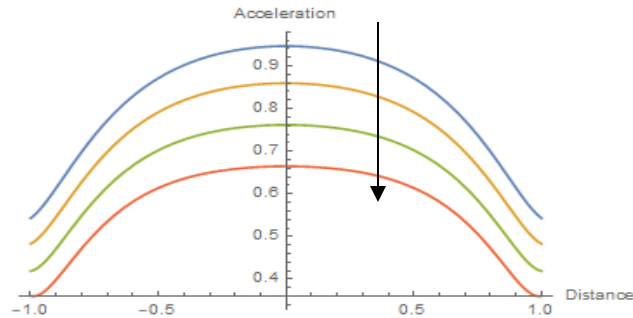


Figure 4.9 Graph for the Blood acceleration with increasing values of Magnetic field $M = 0.75, 1, 1.25, 1.5$, when $Sc = 1, Kr = 1, Gc = 3, Gr = 2, H = 0.5, Pe = 1, Po = 2, Pl = 4, Go = 3, Fr = 0.05, b = 2, \beta = 30^0, k = 0.1, \alpha = 1, h = 1, R = 0.55, \xi = 0.1, \omega = 1, t = 1$.

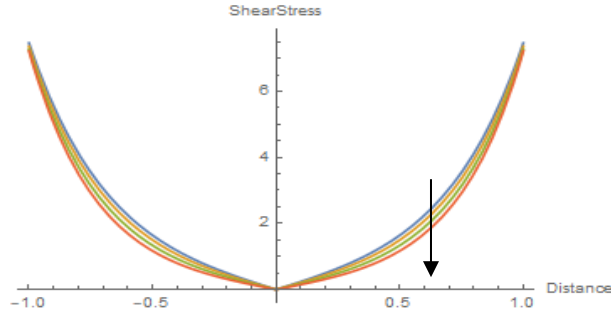


Figure 4.10 Graph for the shear stress at the wall with increasing values of Magnetic field $M = 0.75, 1, 1.25, 1.5$, when $Sc = 1, Kr = 1, Gc = 3, Gr = 2, H = 0.5, Pe = 1, Po = 2, Pl = 4, Go = 3, Fr = 0.05, b = 2, \phi = 30^\circ, \beta = 30^\circ, k = 0.1, \alpha = 1, h = 1, R = 0.55, a = 1, \xi = 0.1, \omega = 1, t = 1$.

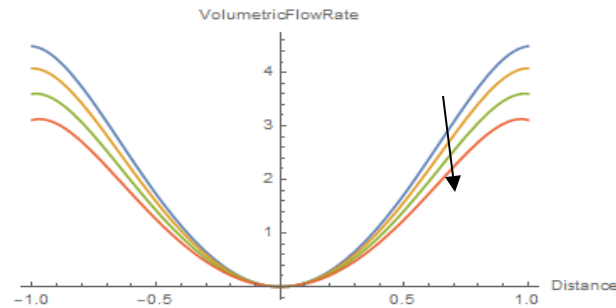


Figure 4.11 Graph for the Volumetric Flow rate with increasing values of Magnetic field $M = 0.75, 1, 1.25, 1.5$, when $Sc = 1, Kr = 1, Gc = 3, Gr = 2, H = 0.5, Pe = 1, Po = 2, Pl = 4, Go = 3, Fr = 0.05, b = 2, \phi = 30^\circ, \beta = 30^\circ, k = 0.1, \alpha = 1, h = 1, R = 0.55, a = 1, \xi = 0.1, \omega = 1, t = 1$.

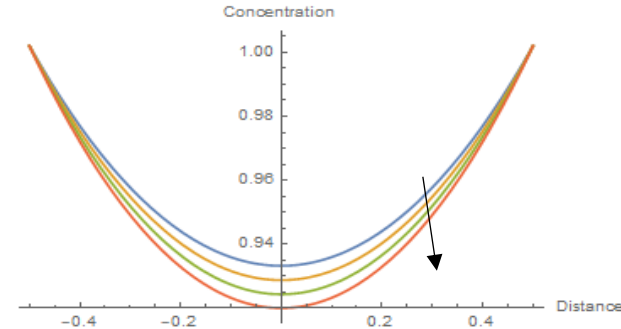


Figure 4.12 Graph for the Concentration with increasing values of Magnetic field $M = 1, 1.5, 2, 2.5$, when $Sc = 1, R = 0.55, Kr = 1, \xi = 0.1, \omega = 1, t = 1$.

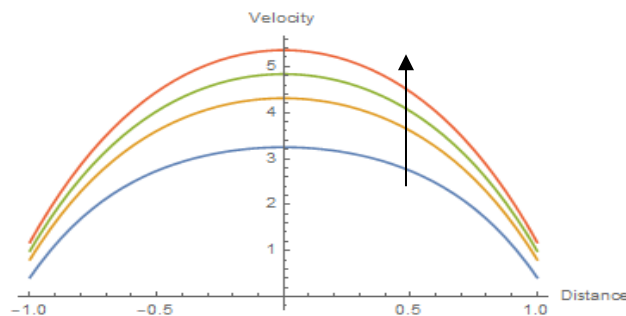


Figure 4.13 Graph for the velocity of Blood flow with increasing values of Permeability of the porous wall $k = 0.5, 1, 2, 3$, when $Sc = 1, Kr = 1, Gc = 3, Gr = 2, H = 0.5, Pe = 1, Po = 2, Pl = 4, Go = 3, Fr = 0.05, b = 2, \phi = 30^\circ, \beta = 30^\circ, \alpha = 1, h = 1, R = 0.55, M = 1.5, \xi = 0.1, \omega = 1, t = 1$.

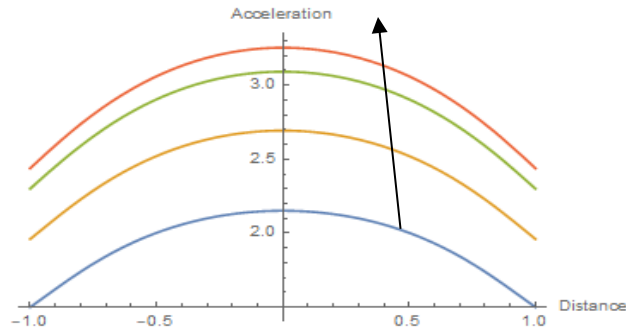


Figure 4.14 Graph for the Blood acceleration with increasing values of Permeability of the porous wall $k = 0.5, 1, 2, 3$, when $Sc = 1, Kr = 1, Gc = 3, Gr = 2, H = 0.5, Pe = 1, Po = 2, Pl = 4, Go = 3, Fr = 0.05, b = 2, \beta = 30^\circ, \alpha = 1, h = 1, R = 0.55, M = 1.5, \xi = 0.1, \omega = 1, t = 1$.

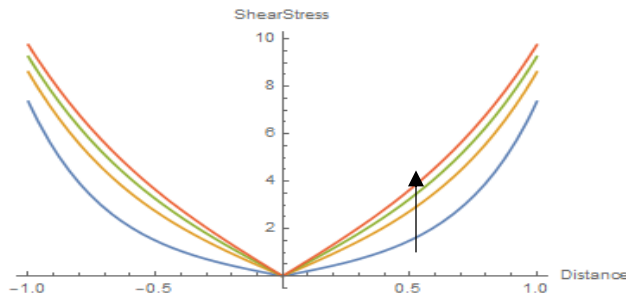


Figure 4.15 Graph for the shear stress at the wall with increasing values of Permeability of the porous wall $k = 0.1, 0.3, 0.5, 1$, when $Sc = 1, Kr = 1, Gc = 3, Gr = 2, H = 0.5, Pe = 1, Po = 2, Pl = 4, Go = 3, Fr = 0.05, b = 2, \phi = 30^\circ, \beta = 30^\circ, \alpha = 1, h = 1, R = 0.55, M = 1.5, a = 1, \xi = 0.1, \omega = 1, t = 1$.

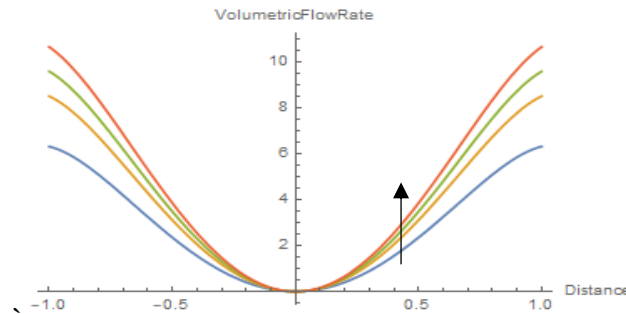


Figure 4.16 Graph for the Volumetric Flow rate with increasing values of Permeability of the porous wall $k = 0.1, 0.3, 0.5, 1$, when $Sc = 1, Kr = 1, Gc = 3, Gr = 2, H = 0.5, Pe = 1, Po = 2, Pl = 4, Go = 3, Fr = 0.05, b = 2, \phi = 30^\circ, \beta = 30^\circ, \alpha = 1, h = 1, R = 0.55, M = 1.5, a = 1, \xi = 0.1, \omega = 1, t = 1$.

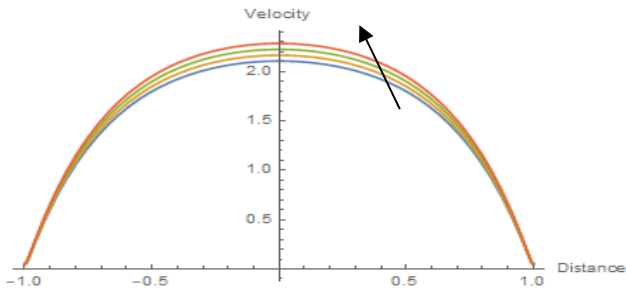


Figure 4.17 Graph for the velocity of Blood flow with increasing values of Pulsatile pressure $Pl = 2, 4, 6, 8$, when $Sc = 1, Kr = 1, Gc = 3, Gr = 2, H = 0.5, Pe = 1, Po = 2, Go = 3, Fr = 0.05, b = 2, \phi = 30^\circ, \beta = 30^\circ, k = 0.1, \alpha = 1, h = 1, R = 0.55, M = 1.5, \xi = 0.1, \omega = 1, t = 1$.

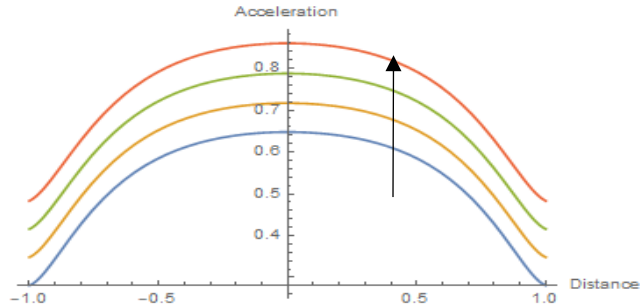


Figure 4.18 Graph for the Blood acceleration with increasing values of Pulsatile pressure $PI = 2, 4, 6, 8$, when $Sc = 1, Kr = 1, Gc = 3, Gr = 2, H = 0.5, Pe = 1, Po = 2, Go = 3, Fr = 0.05, b = 2, \phi = 30^0, \beta = 30^0 k = 0.1, \alpha = 1, h = 1, R = 0.55, M = 1.5, \xi = 0.1, \omega = 1, t = 1$.

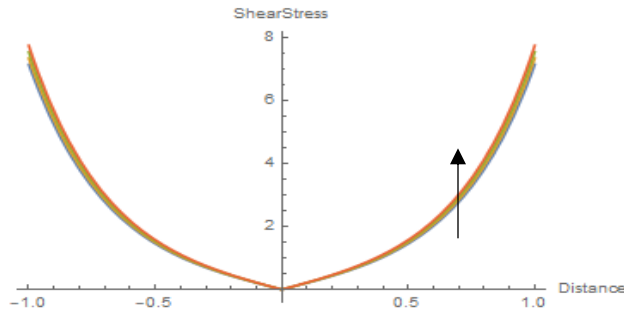


Figure 4.19 Graph for the shear stress at the wall with increasing values of Pulsatile pressure $PI = 2, 4, 6, 8$, when $Sc = 1, Kr = 1, Gc = 3, Gr = 2, H = 0.5, Pe = 1, Po = 2, Go = 3, Fr = 0.05, b = 2, \phi = 30^0, \beta = 30^0 k = 0.1, \alpha = 1, h = 1, R = 0.55, M = 1.5, a = 1, \xi = 0.1, \omega = 1, t = 1$.

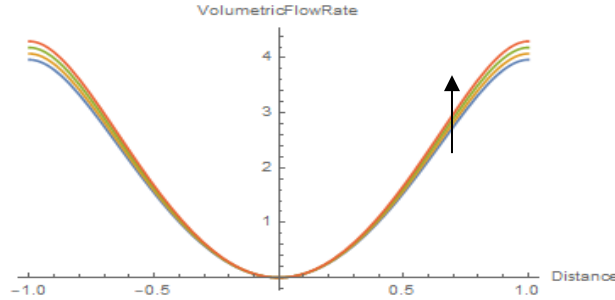


Figure 4.20 Graph for the Volumetric Flow rate with increasing values of Pulsatile pressure $PI = 2, 4, 6, 8$, when $Sc = 1, Kr = 1, Gc = 3, Gr = 2, H = 0.5, Pe = 1, Po = 2, Go = 3, Fr = 0.05, b = 2, \phi = 30^0, \beta = 30^0 k = 0.1, \alpha = 1, h = 1, R = 0.55, M = 1.5, a = 1, \xi = 0.1, \omega = 1, t = 1$.

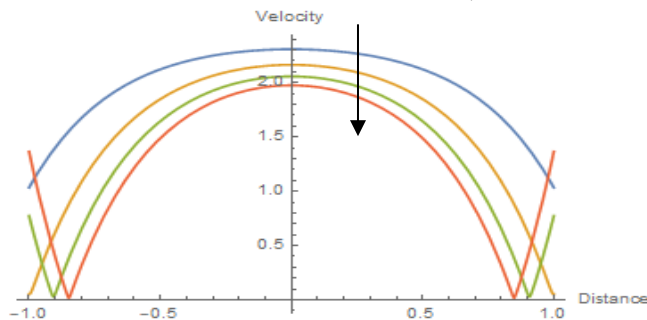


Figure 4.21 Graph for the velocity of Blood flow with increasing values of Slip Parameter $h = 0.5, 1, 1.5, 2$, when $Sc = 1, Kr = 1, Gc = 3, Gr = 2, H = 0.5, Pe = 1, Po = 2, PI = 4, Go = 3, Fr = 0.05, b = 2, \phi = 30^0, \beta = 30^0 k = 0.1, \alpha = 1, R = 0.55, M = 1.5, \xi = 0.1, \omega = 1, t = 1$.

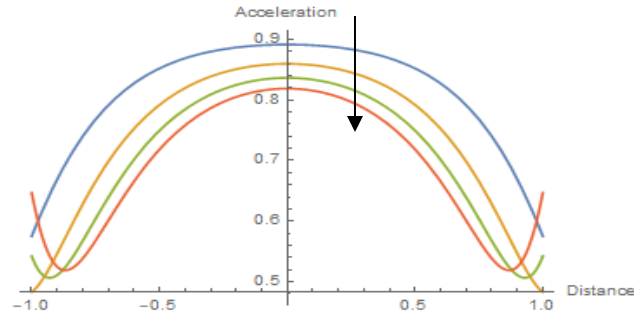


Figure 4.22 Graph for the Blood acceleration with increasing values of Slip Parameter $h = 0.5, 1, 1.5, 2$, when $Sc = 1, Kr = 1, Gc = 3, Gr = 2, H = 0.5, Pe = 1, Po = 2, Pl = 4, Go = 3, Fr = 0.05, b = 2, \beta = 30^\circ, k = 0.1, \alpha = 1, R = 0.55, M = 1.5, \xi = 0.1, \omega = 1, t = 1$

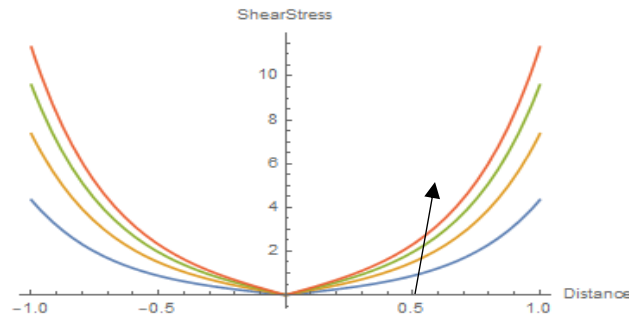


Figure 4.23 Graph for the shear stress at the wall with increasing values of Slip Parameter $h = 0.5, 1, 1.5, 2$, when $Sc = 1, Kr = 1, Gc = 3, Gr = 2, H = 0.5, Pe = 1, Po = 2, Pl = 4, Go = 3, Fr = 0.05, b = 2, \phi = 30^\circ, \beta = 30^\circ, k = 0.1, \alpha = 1, R = 0.55, M = 1.5, a = 1, \xi = 0.1, \omega = 1, t = 1$.

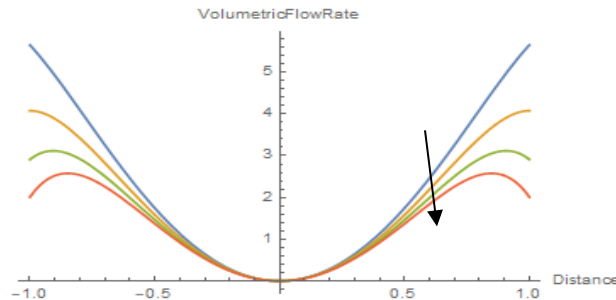


Figure 4.24 Graph for the Volumetric Flow rate with increasing values of Slip Parameter $h = 0.5, 1, 1.5, 2$, when $Sc = 1, Kr = 1, Gc = 3, Gr = 2, H = 0.5, Pe = 1, Po = 2, Pl = 4, Go = 3, Fr = 0.05, b = 2, \phi = 30^\circ, \beta = 30^\circ, k = 0.1, \alpha = 1, R = 0.55, M = 1.5, a = 1, \xi = 0.1, \omega = 1, t = 1$.

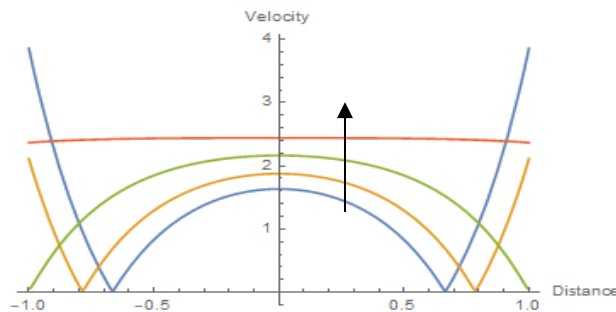


Figure 4.4 Graph for the velocity of Blood flow with increasing values of Radius of stenosis $R = 0.2, 0.3, 0.5, 0.7$, when $Sc = 1, Kr = 1, Gc = 3, Gr = 2, H = 0.5, Pe = 1, Po = 2, Pl = 4, Go = 3, Fr = 0.05, b = 2, \phi = 30^\circ, \beta = 30^\circ, k = 0.1, \alpha = 1, h = 1, M = 1.5, \xi = 0.1, \omega = 1, t = 1$.

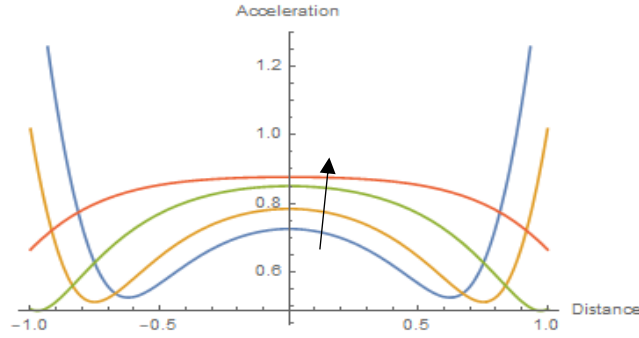


Figure 4.26 Graph for the Blood acceleration with increasing values of Radius of stenosis $R = 0.2, 0.3, 0.5, 0.7$, when $Sc = 1, Kr = 1, Gc = 3, Gr = 2, H = 0.5, Pe = 1, Po = 2, Pl = 4, Go = 3, \beta = 30^\circ, k = 0.1, \alpha = 1, h = 1, M = 1.5, \xi = 0.1, \omega = 1, t = 1$.

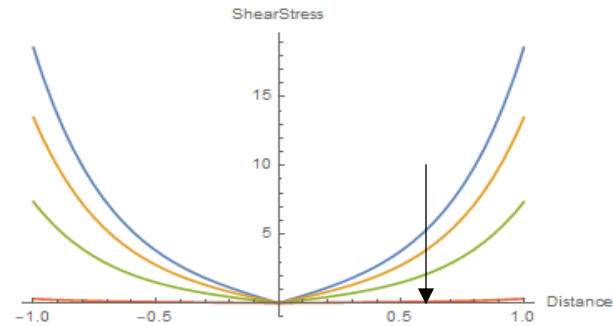


Figure 4.27 Graph for the shear stress at the wall with increasing values of Radius of stenosis $R = 0.2, 0.3, 0.5, 0.7$, when $Sc = 1, Kr = 1, Gc = 3, Gr = 2, H = 0.5, Pe = 1, Po = 2, Pl = 4, Go = 3, Fr = 0.05, b = 2, \phi = 30^\circ, \beta = 30^\circ, k = 0.1, \alpha = 1, h = 1, M = 1.5, a = 1, \xi = 0.1, \omega = 1, t = 1$.

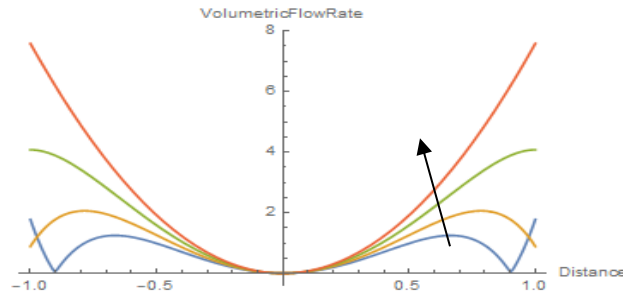


Figure 4.28 Graph for the Volumetric Flow rate with increasing values of Radius of stenosis $R = 0.2, 0.3, 0.5, 0.7$, when $Sc = 1, Kr = 1, Gc = 3, Gr = 2, H = 0.5, Pe = 1, Po = 2, Pl = 4, Go = 3, Fr = 0.05, b = 2, \phi = 30^\circ, \beta = 30^\circ, k = 0.1, \alpha = 1, h = 1, M = 1.5, a = 1, \xi = 0.1, \omega = 1, t = 1$.

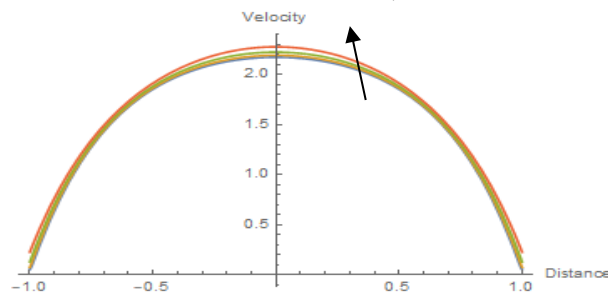


Figure 4.29 Graph for the velocity of Blood flow with increasing values of Heat Source $H = 0.5, 1, 1.5, 2$, when $Sc = 1, Kr = 1, Gc = 3, Gr = 2, Pe = 1, Po = 2, Pl = 4, Go = 3, Fr = 0.05, b = 2, \phi = 30^\circ, \beta = 30^\circ, k = 0.1, \alpha = 1, h = 1, R = 0.55, M = 1.5, \xi = 0.1, \omega = 1, t = 1$.

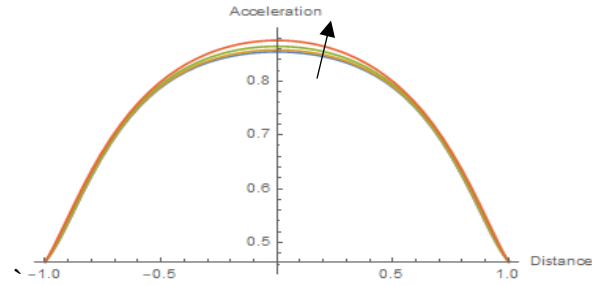


Figure 4.30 Graph for the Blood acceleration with increasing values of Heat Source $H = 0.5, 1, 1.5, 2$, when $Sc = 1, Kr = 1, Gc = 3, Gr = 2, Pe = 1, Po = 2, Pl = 4, Go = 3, b = 2, \beta = 30^\circ, k = 0.1, \alpha = 1, h = 1, R = 0.55, M = 1.5, \xi = 0.1, \omega = 1, t = 1$.

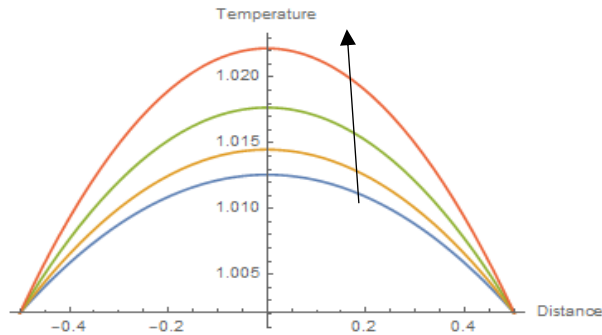


Figure 4.31 Graph for the Temperature with increasing values of Heat Source $H = 0.1, 0.2, 0.3, 0.4$ when $\alpha = 1, R = 0.55, M = 1.5, \xi = 0.1, \omega = 1, t = 1, \theta_a = 1$

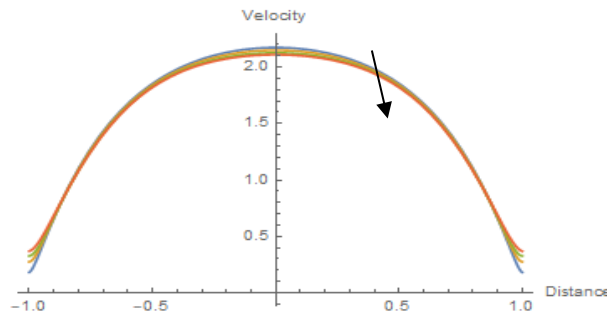


Figure 4.32 Graph for the velocity of Blood flow with increasing values of Peclet number $Pe = 2, 5, 7, 10$, when $Sc = 1, Kr = 1, Gc = 3, Gr = 2, H = 0.5, Po = 2, Pl = 4, Go = 3, Fr = 0.05, b = 2, \phi = 30^\circ, \beta = 30^\circ, k = 0.1, \alpha = 1, h = 1, R = 0.55, M = 1.5, \xi = 0.1, \omega = 1, t = 1$.

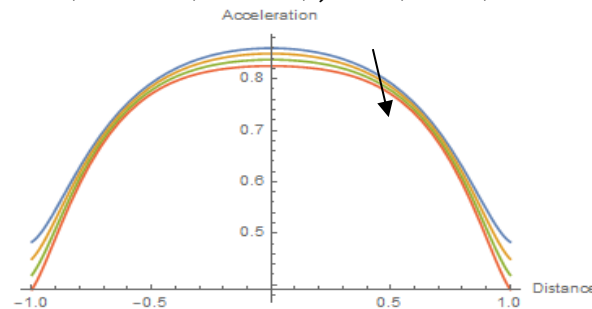


Figure 4.33 Graph for the Blood acceleration with increasing values of Peclet number $Pe = 2, 5, 7, 10$, when $Sc = 1, Kr = 1, Gc = 3, Gr = 2, H = 0.5, Po = 2, Pl = 4, Go = 3, b = 2, \beta = 30^\circ, k = 0.1, \alpha = 1, h = 1, R = 0.55, M = 1.5, \xi = 0.1, \omega = 1, t = 1$.

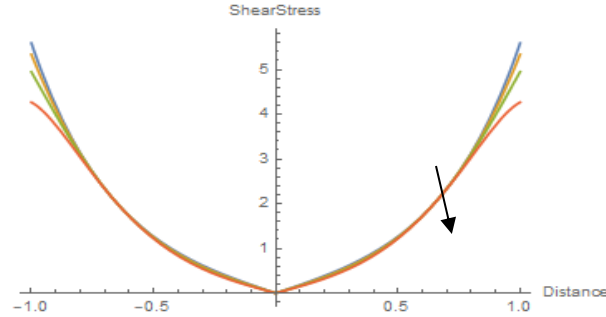


Figure 4.34 Graph for the shear stress at the wall with increasing values of Peclet number $Pe = 2, 5, 7, 10$, when $Gr = 2, H = 0.5, Po = 2, Pl = 4, Go = 3, Fr = 0.05, b = 2, \phi = 30^\circ, \beta = 30^\circ, k = 0.1, \alpha = 1, h = 1, R = 0.55, M = 1.5, a = 1, \xi = 0.1, \omega = 1, t = 1$.

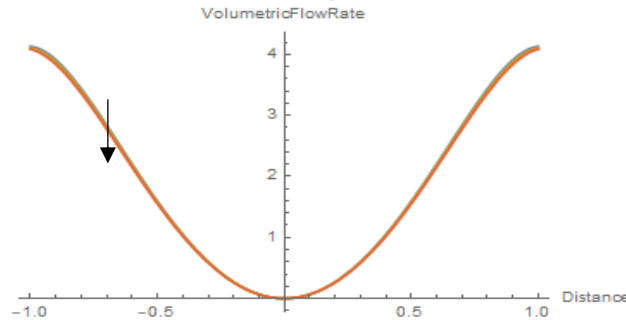


Figure 4.35 Graph for the Volumetric Flow rate with increasing values of Peclet number $Pe = 2, 5, 7, 10$, when $Sc = 1, Kr = 1, Gc = 3, Gr = 2, H = 0.5, Po = 2, Pl = 4, Go = 3, Fr = 0.05, b = 2, \phi = 30^\circ, \beta = 30^\circ, k = 0.1, \alpha = 1, h = 1, R = 0.55, M = 1.5, \xi = 0.1, \omega = 1, t = 1$.

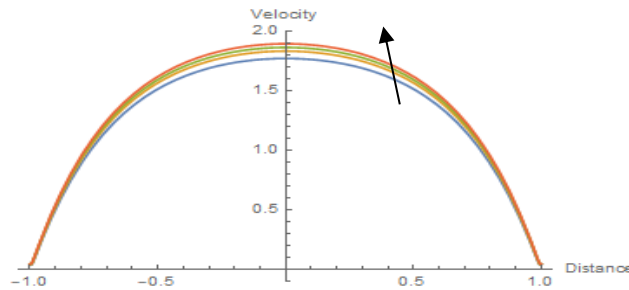


Figure 4.36 Graph for the velocity of Blood flow with increasing values of Grashof temperature number $Gr = 1, 2, 3, 4$, when $Sc = 1, Kr = 1, Gc = 3, H = 0.5, Pe = 1, Po = 2, Pl = 4, Go = 3, Fr = 0.05, b = 2, \phi = 30^\circ, \beta = 30^\circ, k = 0.1, \alpha = 1, h = 1, R = 0.55, M = 1.5, \xi = 0.1, \omega = 1, t = 1$.

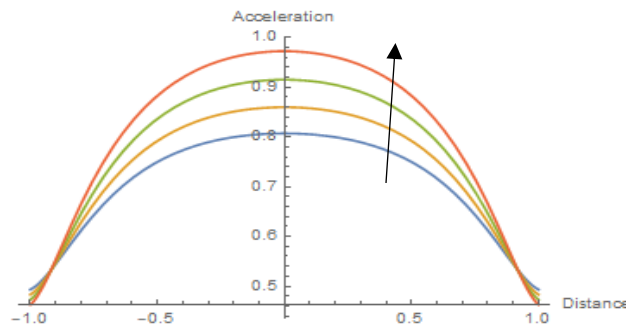


Figure 4.37 Graph for the Blood acceleration with increasing values of Grashof temperature number $Gr = 1, 2, 3, 4$, when $Sc = 1, Kr = 1, Gc = 3, H = 0.5, Pe = 1, Po = 2, Pl = 4, Go = 3, Fr = 0.05, b = 2, \phi = 30^\circ, \beta = 30^\circ, k = 0.1, \alpha = 1, h = 1, R = 0.55, M = 1.5, \xi = 0.1, \omega = 1, t = 1$.

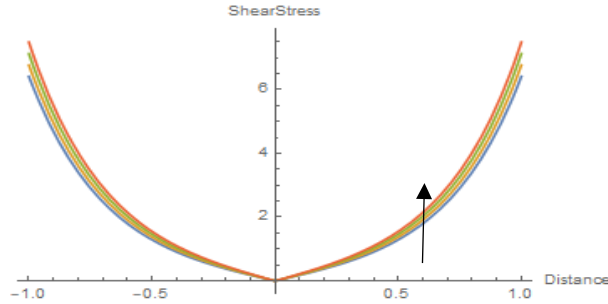


Figure 4.38 Graph for the shear stress at the wall with increasing values of Grashof temperature number $Gr = 1, 2, 3, 4$, when $Sc = 1, Kr = 1, Gc = 3, H = 0.5, Pe = 1, Po = 2, Pl = 4, Go = 3, Fr = 0.05, b = 2, \phi = 30^\circ, \beta = 30^\circ, k = 0.1, \alpha = 1, h = 1, R = 0.55, M = 1.5, a = 1, \xi = 0.1, \omega = 1, t = 1$.

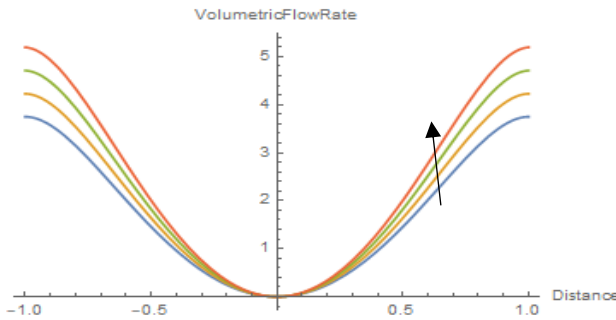


Figure 4.39 Graph for the Volumetric Flow rate with increasing values of Grashof temperature number $Gr = 1, 2, 3, 4$, when $Sc = 1, Kr = 1, Gc = 3, H = 0.5, Pe = 1, Po = 2, Pl = 4, Go = 3, Fr = 0.05, b = 2, \phi = 30^\circ, \beta = 30^\circ, k = 0.1, \alpha = 1, h = 1, R = 0.55, M = 1.5, \xi = 0.1, \omega = 1, t = 1$.

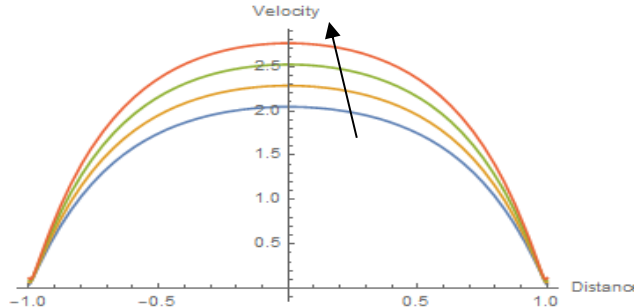


Figure 4.40 Graph for the velocity of Blood flow with increasing values of Grashof Diffusion number $Gc = 1, 2, 3, 4$, when $Sc = 1, Kr = 1, Gr = 2, H = 0.5, Pe = 1, Po = 2, Pl = 4, Go = 3, Fr = 0.05, b = 2, \phi = 30^\circ, \beta = 30^\circ, k = 0.1, \alpha = 1, h = 1, R = 0.55, M = 1.5, \xi = 0.1, \omega = 1, t = 1$.

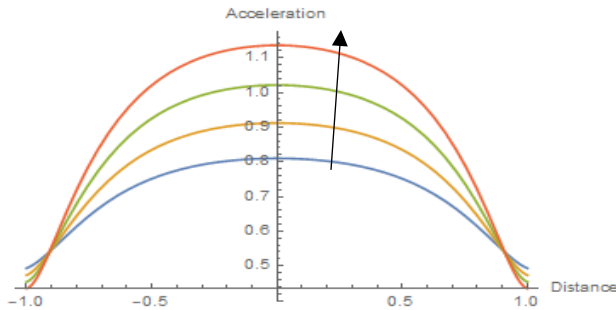


Figure 4.41 Graph for the Blood acceleration with increasing values of Grashof Diffusion number $Gc = 1, 2, 3, 4$, when $Sc = 1, Kr = 1, Gr = 2, H = 0.5, Pe = 1, Po = 2, Pl = 4, Go = 3, b = 2, \beta = 30^\circ, k = 0.1, \alpha = 1, h = 1, R = 0.55, M = 1.5, \xi = 0.1, \omega = 1, t = 1$.

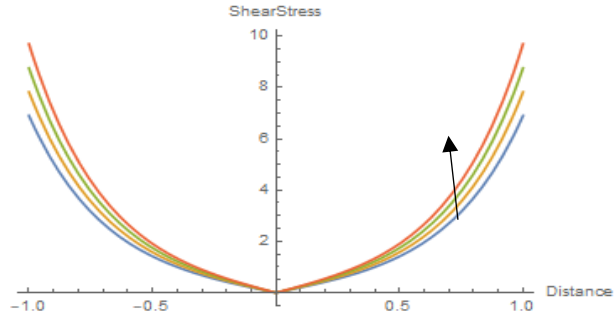


Figure 4.42 Graph for the shear stress at the wall in the third consideration with increasing values of Grashof Diffusion number $G_c = 1, 2, 3, 4$, when $Sc = 1, Kr = 1, Gr = 2, H = 0.5, Pe = 1, Po = 2, Pl = 4, Go = 3, Fr = 0.05, b = 2, \phi = 30^\circ, \beta = 30^\circ, k = 0.1, \alpha = 1, h = 1, R = 0.55, M = 1.5, a = 1, \xi = 0.1, \omega = 1, t = 1$.

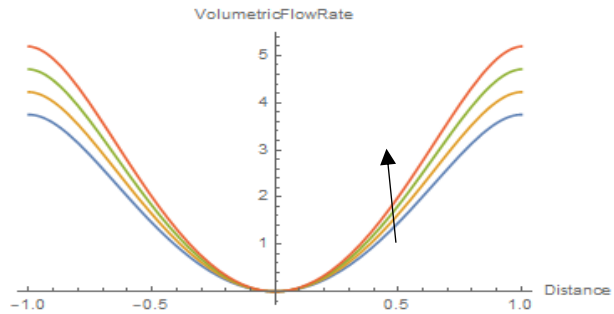


Figure 4.43 Graph for the Volumetric Flow rate with increasing values of Grashof Diffusion number $G_c = 1, 2, 3, 4$, when $Sc = 1, Kr = 1, Gr = 2, H = 0.5, Pe = 1, Po = 2, Pl = 4, Go = 3, Fr = 0.05, b = 2, \phi = 30^\circ, \beta = 30^\circ, k = 0.1, \alpha = 1, h = 1, R = 0.55, M = 1.5, \xi = 0.1, \omega = 1, t = 1$.

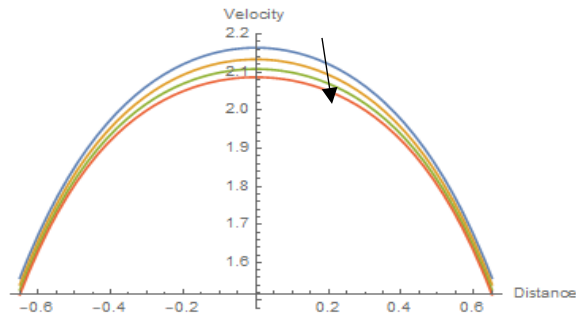


Figure 4.44 Graph for the velocity of Blood flow with increasing values of Chemical Reaction $Kr = 1, 3, 5, 7$, when $Sc = 1, G_c = 3, Gr = 2, H = 0.5, Pe = 1, Po = 2, Pl = 4, Go = 3, Fr = 0.05, b = 2, \phi = 30^\circ, \beta = 30^\circ, k = 0.1, \alpha = 1, h = 1, R = 0.55, M = 1.5, \xi = 0.1, \omega = 1, t = 1$.

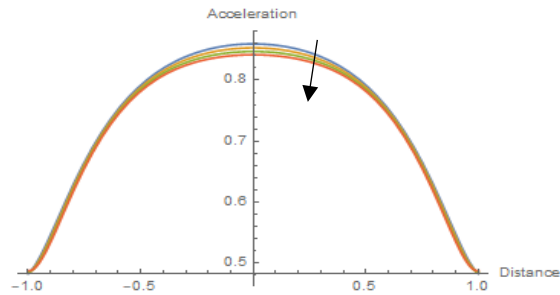


Figure 4.45 Graph for the Blood acceleration with increasing values of Chemical Reaction $Kr = 1, 3, 5, 7$, when $Sc = 1, G_c = 3, Gr = 2, H = 0.5, Pe = 1, Po = 2, Pl = 4, Go = 3, b = 2, \beta = 30^\circ, k = 0.1, \alpha = 1, h = 1, R = 0.55, M = 1.5, \xi = 0.1, \omega = 1, t = 1$.

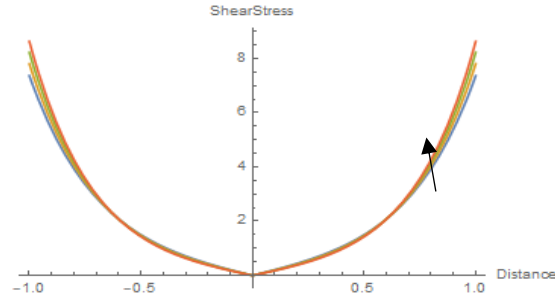


Figure 4.46 Graph for the shear stress at the wall with increasing values of Chemical Reaction $Kr = 1, 3, 5, 7$, when $Sc = 1, Gc = 3, Gr = 2, H = 0.5, Pe = 1, Po = 2, Pl = 4, Go = 3, Fr = 0.05, b = 2, \phi = 30^0, \beta = 30^0 k = 0.1, \alpha = 1, h = 1, R = 0.55, M = 1.5, a = 1, \xi = 0.1, \omega = 1, t = 1$.

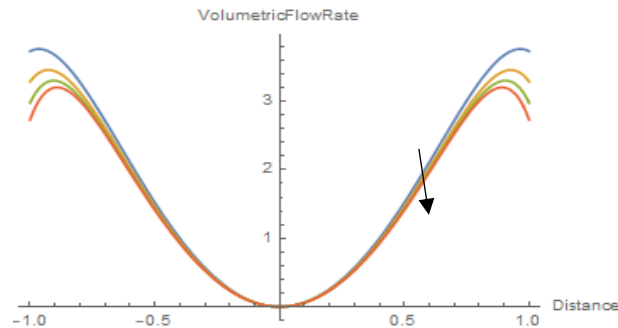


Figure 4.47 Graph for the Volumetric Flow rate with increasing values of Chemical Reaction $Kr = 1, 3, 5, 7$, when $Sc = 1, Gc = 3, Gr = 2, H = 0.5, Pe = 1, Po = 2, Pl = 4, Go = 3, Fr = 0.05, b = 2, \phi = 30^0, \beta = 30^0 k = 0.1, \alpha = 1, h = 1, R = 0.55, M = 1.5, \xi = 0.1, \omega = 1, t = 1$.

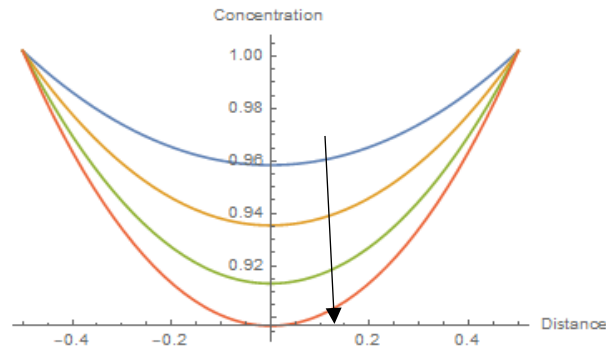


Figure 4.48 Graph for the Concentration with increasing values of Chemical reaction $Kr = 1, 2, 3, 4$, when $Sc = 1, R = 0.55, M = 1.5, \xi = 0.1, \omega = 1, t = 1$.

III. CONCLUSION

Conclusively, the results gotten with graphical illustration showed that,

1. The increase in the Magnetic field decreased the blood flow velocity because persistent rotating motion of the blood increases internal viscosity of the red blood cells (RBC) which increases the Lorentz force that inhibits the blood flow. This also decreases the acceleration of the blood, shear stress at the artery wall and the volumetric flow rate for all the considerations. Also, the increase in the magnetic field increased the temperature at the center before converging to zero at the wall but decreased the concentration profile.

2. The increase in the body acceleration increases the blood flow velocity because of the reduced resistance to blood flow which causes increased pulse rate and heart beat resulting to increased blood flow to the muscles from the heart. This also increases the blood acceleration, shear stress at the artery wall and the volumetric flow rate for all the considerations.
3. The increase in the slip decreased the blood flow velocity because of relative movement between the blood and the artery wall. This in turn causes the decrease in the blood acceleration and the volumetric flow rate but increases the shear stress at the artery wall for all considerations.
4. The increase in the pulsatile pressure results to an increase in the velocity of the blood flow because the heart work rate increases due to more blood been pumped from the heart to muscles in the body. This will result to an increase in the blood acceleration, volumetric flow rate and shear stress at the artery wall for all considerations.
5. The increase in the heat source caused an increase in the velocity of the blood flowing axially because it slightly decreases the internal viscosity of the red blood cells (RBC). This results to an increase in the blood acceleration and volumetric flow rate but a decrease in the shear stress at the wall for all consideration.
6. The increase in the inclination of the artery created irregular pattern on the blood flow for each consideration. For the first consideration the blood flow velocity increased, for the second it was irregular and then for the third consideration, it decreased. An increase in the inclination of the artery caused the volumetric flow rate and the shear stress at the wall to increase for the first and second consideration but an irregular behavior in the third consideration for both the volumetric flow rate and the shear stress at the artery wall.
7. The increase in the artery radius with stenosis caused an increase in the blood flow velocity, blood acceleration, and volumetric flow rate but a decrease in the shear stress at the wall for all consideration.
8. An increase in the Grashof temperature number increased the blood flow velocity, blood acceleration, shear stress at the wall and the volumetric flow rate for the second and third consideration.
9. An increase in the Grashof diffusion number increased the blood flow velocity, blood acceleration, shear stress at the artery wall and the volumetric flow rate for the second and third consideration.
10. An increase in the chemical reaction decreased the blood flow velocity, blood acceleration and the volumetric flow rate but increases the shear stress at the artery wall. Also, the increase in the chemical reaction decreased the concentration profile.

REFERENCES

- [1] Blessy, T. & Sumam, K. S. (2016). Blood Flow in Human Arterial System-A Review. *Procedia Technology*, Volume 24, Pages 339-346, ISSN 2212-0173, <https://doi.org/10.1016/j.protcy.2016.05.045>.
- [2] Ku, D. N. (2021). Blood Flow in arteries. *Annual Reviews of Fluid Mechanics*, Volume 21, Issue 1, 0066-4189, doi: 10.1146/annurev.fluid.29.1.399.
- [3] Allen, G. S., Murray, K. D. & Olsen, D. B. (1997). The importance of pulsatile and nonpulsatile flow in the design of blood pumps. *Artif. Organs*. Aug 21(8):922-8, doi: 10.1111/j.1525-1594.1997.tb00252.x. PMID: 9247182.
- [4] Pellerito, J. S. (2020). The Hemodynamics of Vascular Disease. In *Introduction to Vascular Ultrasonography*, 2020.
- [5] Sanka, D. S. (2010). Pulsatile Flow of Two-Fluid Model of Blood Flow through Arteria Stenosis. *Mathematical Problem in Engineering*, Volume 2010, Page 26, doi:10.1155/2010/465835
- [6] Nehad, A. S., Al-Zubaidi, A. & Saleem, S. (2021). Study of Magneto Hydrodynamic Pulsatile Blood Flow through an Inclined Porous Cylindrical Tube with Generalized Time Non-Local Shear Stress. *Advances in Mathematical Physics*, Volume 2021, Page 11, <https://doi.org/10.1155/2021/5546701>
- [7] Lukendra, K., Druba, P. B., Nazibuddin, A. & Karabi, D. C. (2017). MHD Pulsatile Slip Flow of Blood through Porous Medium in an Inclined Stenosed Tapered Artery in Presence of Body Acceleration. *Advances in Theoretical and Applied Mathematics* ISSN 0973-4554 Volume 12, Number 1 (2017), pp. 15-38
- [8] Eldesoky, M. I. (2012). Slip Effects on the Unsteady MHD Pulsatile Blood Flow through Porous Medium in an Artery under the Effect of Body Acceleration. *International Journal of Mathematics and Mathematical Sciences*, Volume 2012, 26 pages doi:10.1155/2012/860239
- [9] Das, K. & Saha, G. C. (2009). Arterial MHD Pulsatile Flow of Blood under Periodic Body Acceleration. *Bull. Soc. Math. Banja Luka*, ISSN 0354-5792, Vol. 16 (2009), 21-42.
- [10] Varun, K. T., Varshney, N. K. & Agarwal, R. (2016). Effect of body acceleration on pulsatile blood flow through a catheterized artery. *Advances in Applied Science Research*, 7(2):155-166, <http://www.pelagiaresearchlibrary.com/>.
- [11] Prakash, O., Singh, S. P., Kumar, D. & Dwivedi, Y. K. (2011). A study of effects of heat source on MHD blood flow through bifurcated arteries. *AIP Advances*, Volume 1, Issue 4, 10.1063/1.365861
- [12] Kumar, B., Satyanarayana, B., Kumar, R., Kumar, S. & Deo, N. (2021). Application of heat source and chemical reaction in MHD blood flow through permeable bifurcated arteries with inclined magnetic field in tumor treatments. *Results in Applied Mathematics*, 10, 100151.
- [13] Omamoke, E. & Amos, E. (2020). The Impact of Chemical Reaction and Heat source on MHD Free Convection Flow over an Inclined Porous Surface. *International Journal of Scientific and Research Publications*, Volume 10, Issue 5, ISSN 2250-3153, DOI: 10.29322/IJSRP.10.05.2020.p10103
- [14] Omamoke, E., Amos, E., & Jafari, E. (2020). Impact of Thermal Radiation and Heat Source on MHD Blood Flow with an Inclined Magnetic Field in Treating Tumor and Low Blood Pressure. *Asian Research Journal of Mathematics*, 16(9), 77-87. <https://doi.org/10.9734/arjom/2020/v16i930221>.

- [15] Omamoke, E. & Amos, E. (2020). Chemical Reaction, Radiation and Heat Source Effects on Unsteady MHD Blood Flow Over a Horizontal Porous Surface in the Presence of an Inclined Magnetic Field. *International Journal of Scientific & Engineering Research*, Volume 11, Issue 4, April-2020 ISSN 2229-5518.
- [16] Sinha, A., Shit, G. C. & Kundu, P. K. (2013). Slip Effect on Pulsatile Flow of Blood through a Stenosed Arterial Segment under Periodic Body Acceleration. *ISRN Biomedical Engineering*, doi.org/10.1155/2013/925876.
- [17] Nandal, J. & Kumari, S. (2019). The effect of slip velocity on unsteady peristalsis MHD blood flow through a constricted artery experiencing body acceleration. *International Journal of Applied Mechanics and Engineering*, Volume 24, No. 3, pp. 645-659.
- [18] Sharma, M., Gaur, R. K. & Biswas, P. (2018). Effect of slip parameter on MHD blood flow and heat transfer through a porous medium with variable viscosity. *International Journal of engineering sciences and research*, 7(4), DOI:10.5281/zenodo.1228826, ISSN: 2277-9655.
- [19] Kumar, A., Chandel, R. S., Shrivastava, R., Shrivastava, K. & Kumar, S. (2016). Mathematical Modelling of blood flow in an inclined tapered artery under MHD effect through porous medium. *International Journal of Pure and Applied Mathematical Science*, 9(1), 75 – 88, ISSN 0972 – 9828.
- [20] Sinha, A., Shit, G. C. & Kundu, P. K. (2013). Slip Effect on Pulsatile Flow of Blood through a Stenosed Arterial Segment under Periodic Body Acceleration. *ISRN Biomedical Engineering*, doi.org/10.1155/2013/925876.
- [21] Amos, E. & Ogulu, A. (2003). Magnetic Effect on Pulsatile Flow in a Constricted Axis-symmetric Tube. *Indian Journal Pure and Applied Mathematics*, 34 (9): 1315-1326, September.
- [22] Nandal, J. & Kumari, S. (2019) Nadeem, S., Noreen, S. A., Hayat, T. & Awatif, A. H. (2012). Influence of Heat and Mass Transfer on Newtonian Bio magnetic Fluid of Blood Flow through a Tapered Porous Artery with Stenosis. *Transport in Porous Medium*, 91(1):81-100.
- [23] Bunonyo, W. K. and Amos, E. 2020. Lipid concentration effect on blood flow through an inclined arterial channel with magnetic field. *Mathematical modelling and Applications*, 5(3), 129 – 137.

APPENDIX

$$S_4 = \frac{G_r C_1 N^8 + G_c C_3 K r^4}{\beta_1 2^2 4^2 6^2 8^2}$$

$$S_3 = \frac{1}{\beta_1} \left(64 S_4 - \left(\frac{G_r C_1 N^6 - G_c C_3 K r^3}{2^2 4^2 6^2} \right) \right)$$

$$S_2 = \frac{1}{\beta_1} \left(36 S_3 + \left(\frac{(G_r C_1 N^4 + G_c C_3 K r^2)}{2^2 4^2} \right) \right)$$

$$S_1 = \frac{1}{\beta_1} \left(16 S_2 - \left(\frac{G_r C_1 N^2 - G_c C_3 K r}{2^2} \right) \right)$$

$$S_0 = \frac{1}{\beta_1} (4 S_1 + G + G_r C_1 + G_c C_3)$$

$$T_4 = \frac{G_r C_2 \alpha_1^4 + G_c C_4 \alpha_2^3}{\beta_2 2^2 4^2 6^2 8^2}$$

$$T_3 = \frac{1}{\beta_2} \left(64 T_4 - \left(\frac{G_r C_2 \alpha_1^3 - G_c C_4 \alpha_2^3}{2^2 4^2 6^2} \right) \right)$$

$$T_2 = \frac{1}{\beta_2} \left(36 T_3 + \left(\frac{(G_r C_2 \alpha_1^2 + G_c C_4 \alpha_2^2)}{2^2 4^2} \right) \right)$$

$$T_1 = \frac{1}{\beta_2} \left(16 T_2 - \left(\frac{G_r C_2 \alpha_1 - G_c C_4 \alpha_2}{2^2} \right) \right)$$

$$T_0 = \frac{1}{\beta_2} (4 T_1 + F + G_r C_2 + G_c C_4)$$